Part 2: Survey of parameterizations

- Vertical (diapycnal) mixing
- Bottom boundary layers and topographic effects
- Lateral (isopycnal) mixing
- Eddy induced velocities and other dynamical effects of eddies

MERSEA 1 models

	PSY2	FOAM	MSF-MOM	MSF-OPA
δt	800s	1200s	900s	600S
δx max,min	7 km 3 km	12 km 12 km	12 km 9.8 km	6 km 4.9 km
levels	43	20	31	72
δz min	6 m	10 m	10 m	3 m
LBC	Partial slip	No slip	No slip	No slip

1 – Convection and interior mixing

	PSY2	FOAM	MSF1	MFS2
ν_T (m^2s^{-1})	10^{-5}		3.10^{-5}	3.10^{-5}
	TKE +surf	PP81, KPP,KT67		
ν_m (m^2s^{-1})	10^{-4}		1.510^{-4}	1.510^{-4}
	TKE	PP81, KPP,KT67		
Convection		Adjust.	Adjust.	
ν_c (m^2s^{-1})	1			1

Convection

Problems with the convection algorithms

(Killworth, 1989)

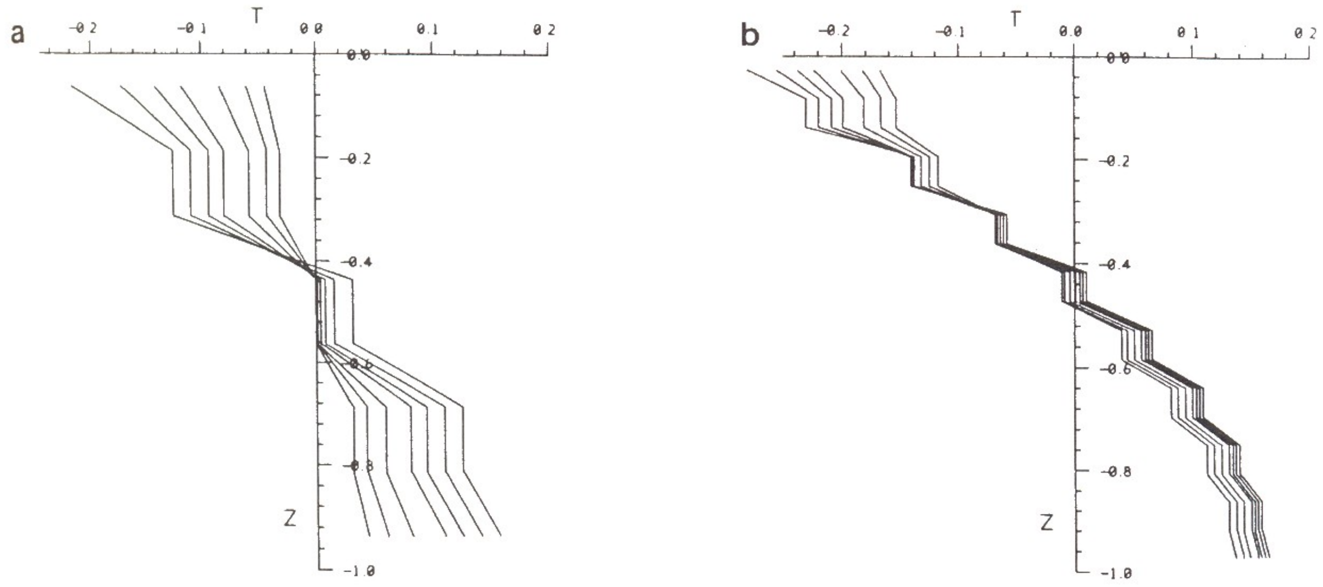

Fig. 3. Steady solution to the simple convection problem (1) to (4), using NCON passes of the standard convection algorithm. Reading from left to right at the top, NCON = 1, 2, 3, 4, 6, 8, 10. (The correct solution is identically zero.) (a) using 8 grid points; (b) using 18 grid points.

Convection = mixing

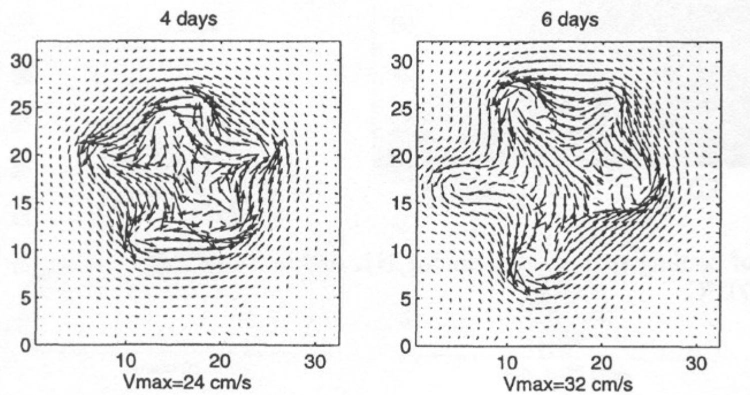

Figure 8. Velocity fields, experiment S, depth of 112 m, days 4 and 6.

Stratified convection with a non-hydrostatic model. (Klinger, Marshall and Send, 1996).

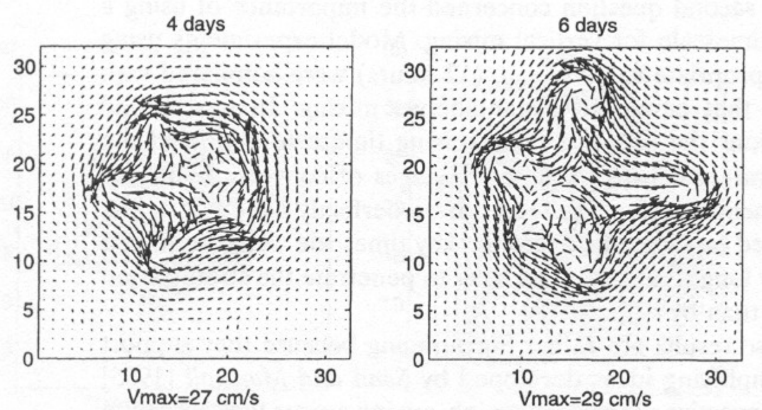

Figure 9. Velocity fields, experiment SF, depth of 112 m, days 4 and 6

Stratified convection with a vertical mixing of 9 m²/s.

Mixing of tracers, momentum?

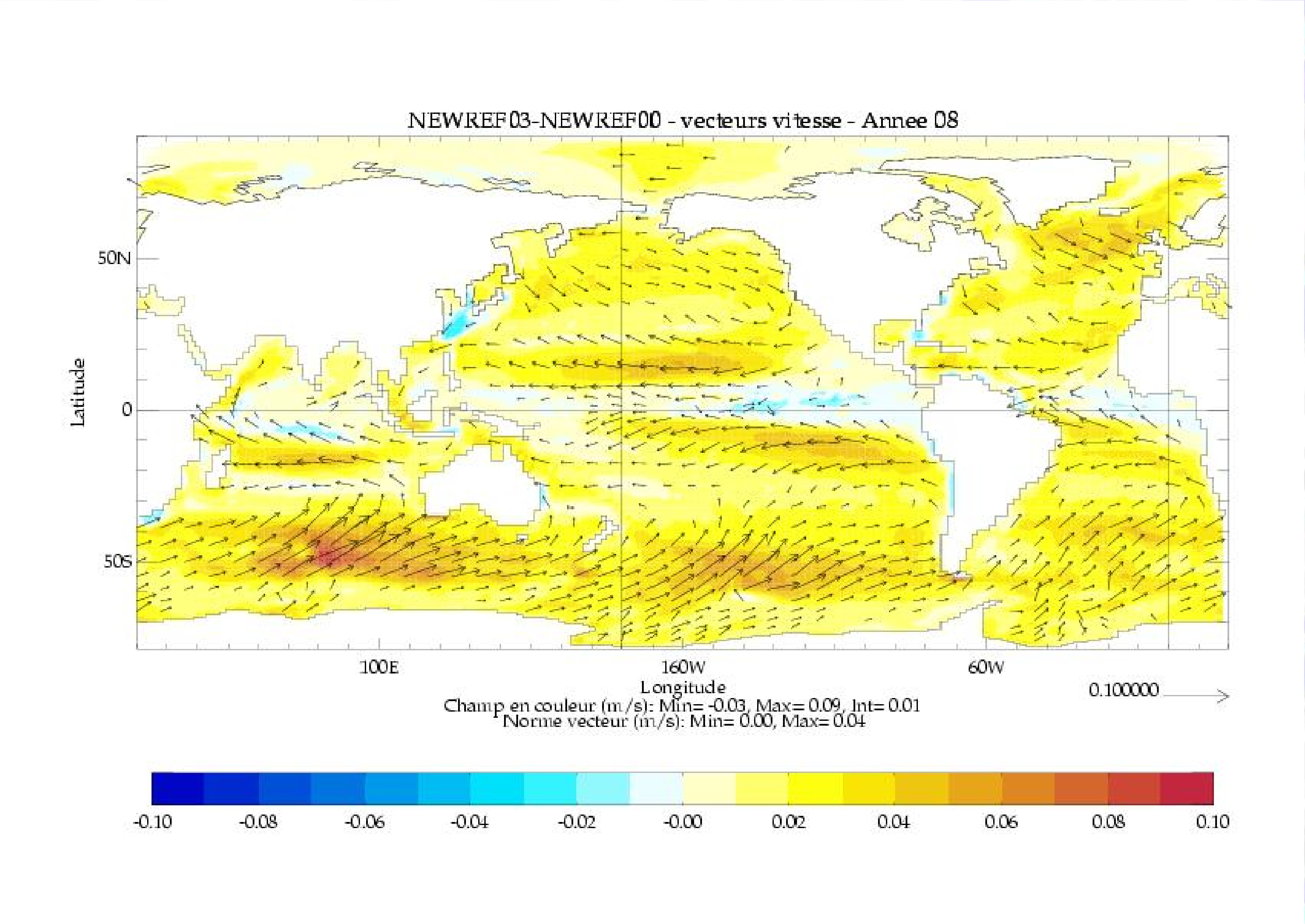

Matteoli and Madec 2003, ORCA2 model, 8 years run

Mixing packages

Parameterizations from turbulent closures or KPP deal with both the surface mixed layer and Richardson-dependent mixing in the interior.

KPP: K-profile in the surface mixed layer

simple nonlinear function of Ri in the interior

TKE: local, complex function of Ri everywhere

Mersea 1 parameterizations

	PSY2	FOAM	MSF1	MFS2
ν_T (m^2s^{-1})	10^{-5}		3.10^{-5}	3.10^{-5}
	TKE +surf	PP81, KPP,KT67		
ν_m (m^2s^{-1})	10^{-4}		1.510^{-4}	1.510^{-4}
	TKE	PP81, KPP,KT67		
Convection		Adjust.	Adjust.	
ν_c (m^2s^{-1})	1			1
Bottom fric	$1.3\ 10^{-3}$	$1.225\ 10^{-3}$	none	$1.\ 10^{-3}$

KPP- TKE comparison

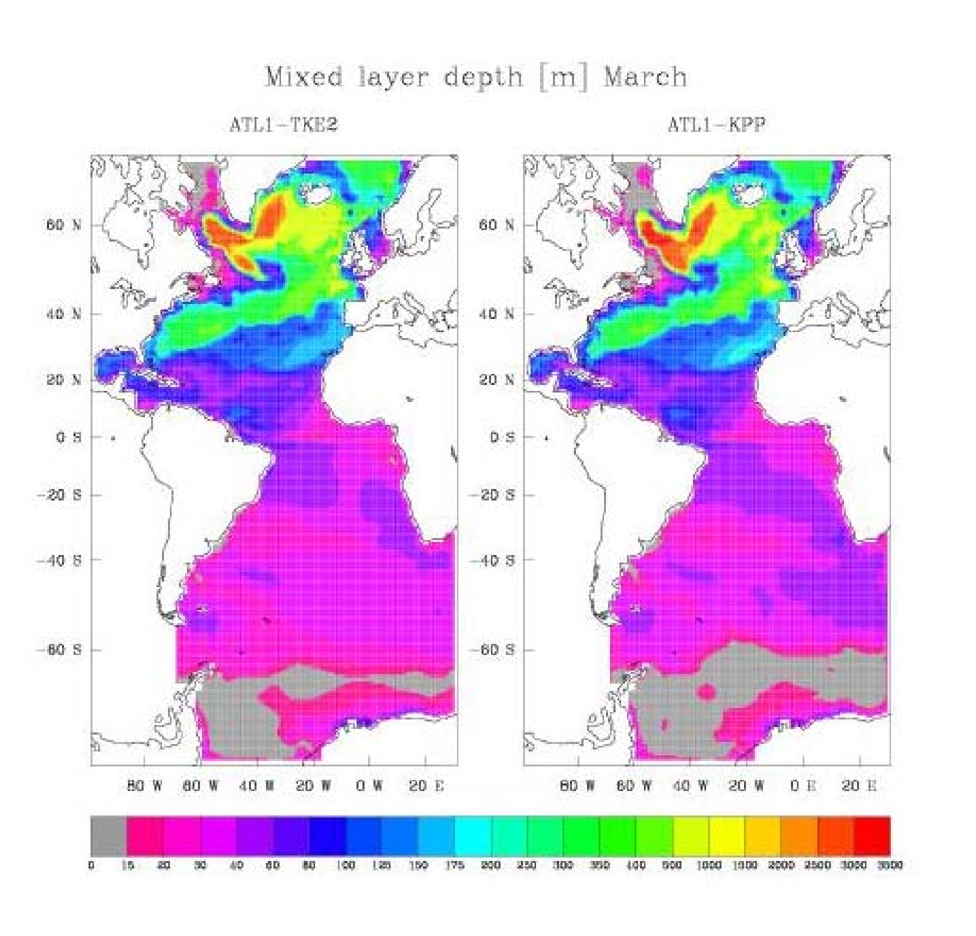

Chanut, 2004: comparison in the CLIPPER ATL1 model. Differences are small.

Surface mixed layer/interior

Model of the flow of Antarctic bottom water in the Romanche fracture zone (OPA model, 5 km /50m resolution, TKE parameterization; Bruno Ferron, 2001)

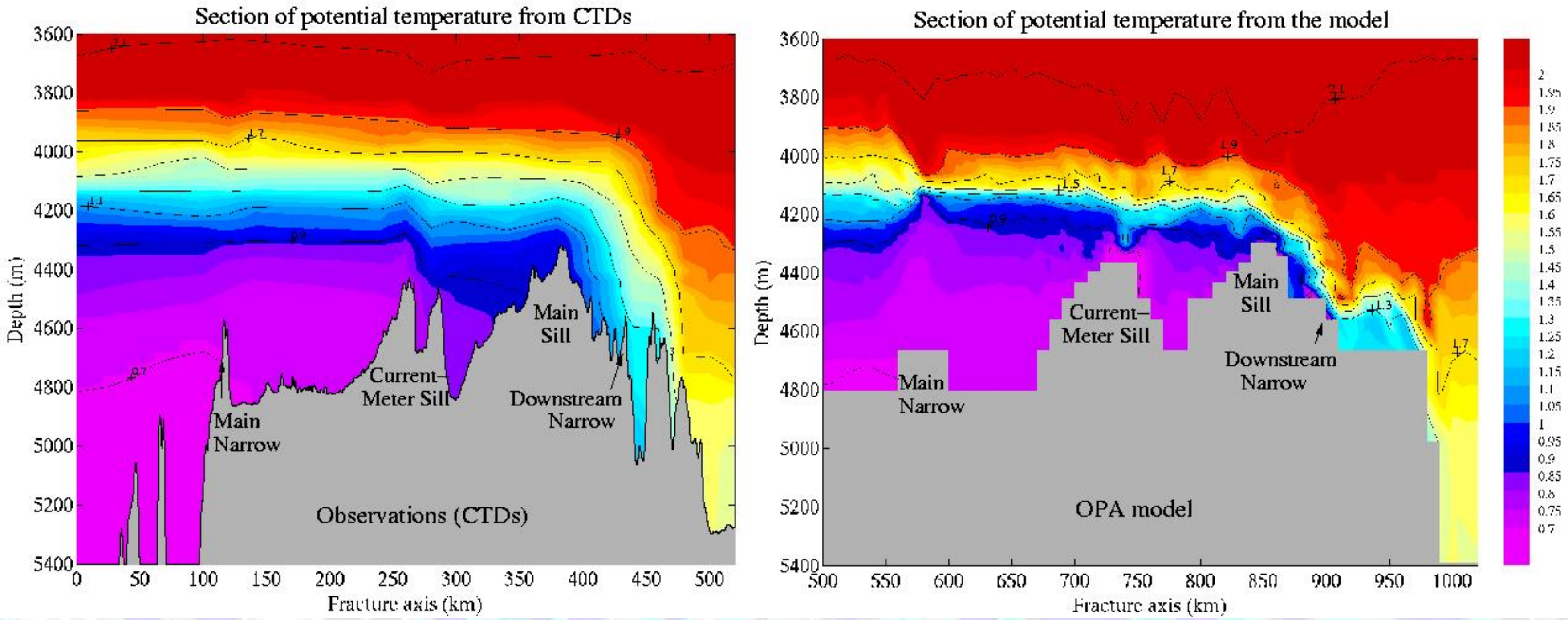

Measurements of vertical mixing

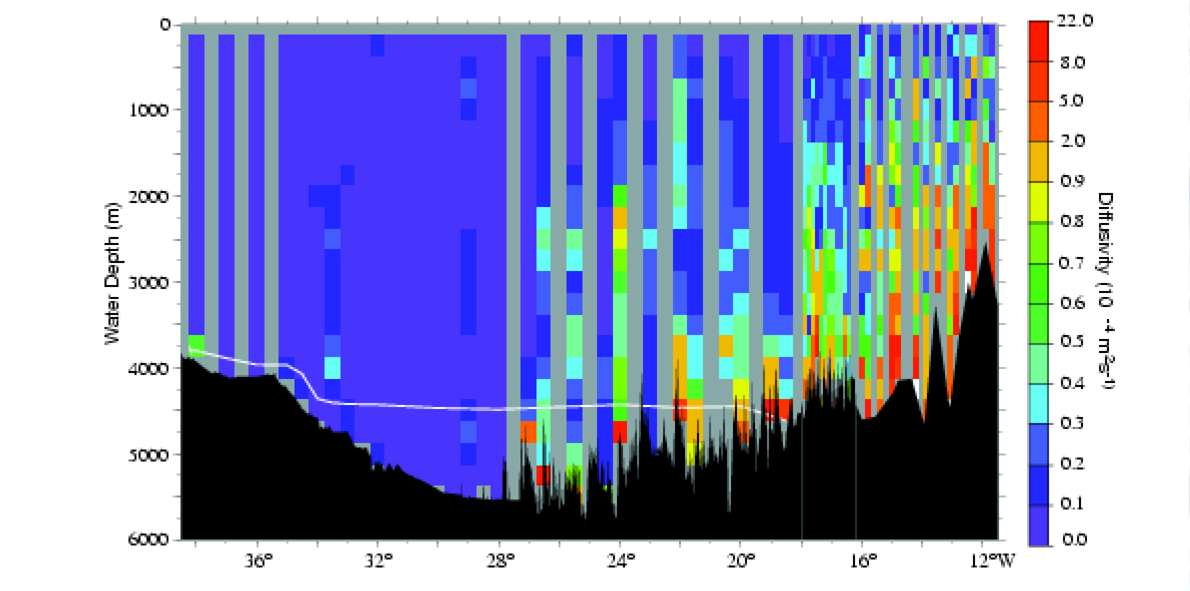

Toole et al, 1997: Depth-longitude section of cross-isopycnal diffusivity in the Brazil Basin from velocity microstructure obervations. White line is the 0.8° temperature contour.

Interior mixing: tidal forcing

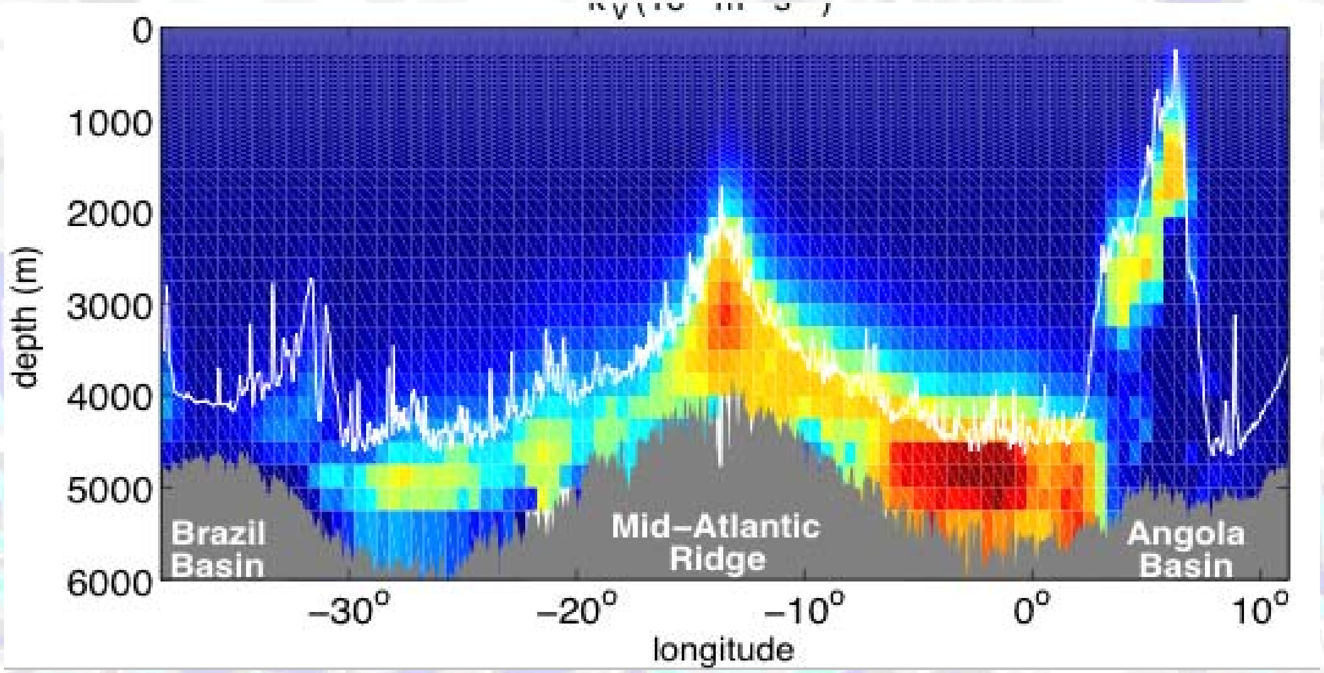

parameterization of Jayne et al, used by Simmons et al. (2004) in an OGCM.

Interior mixing: numerical issues

With low resolution models, diapycnal mixing when WBC not well resolved

With eddy resolving model, diapycnal mixing when the variance cascading to the grid scale is not handled properly

(Griffies et al 2000)

Numerical diapycnal mixing

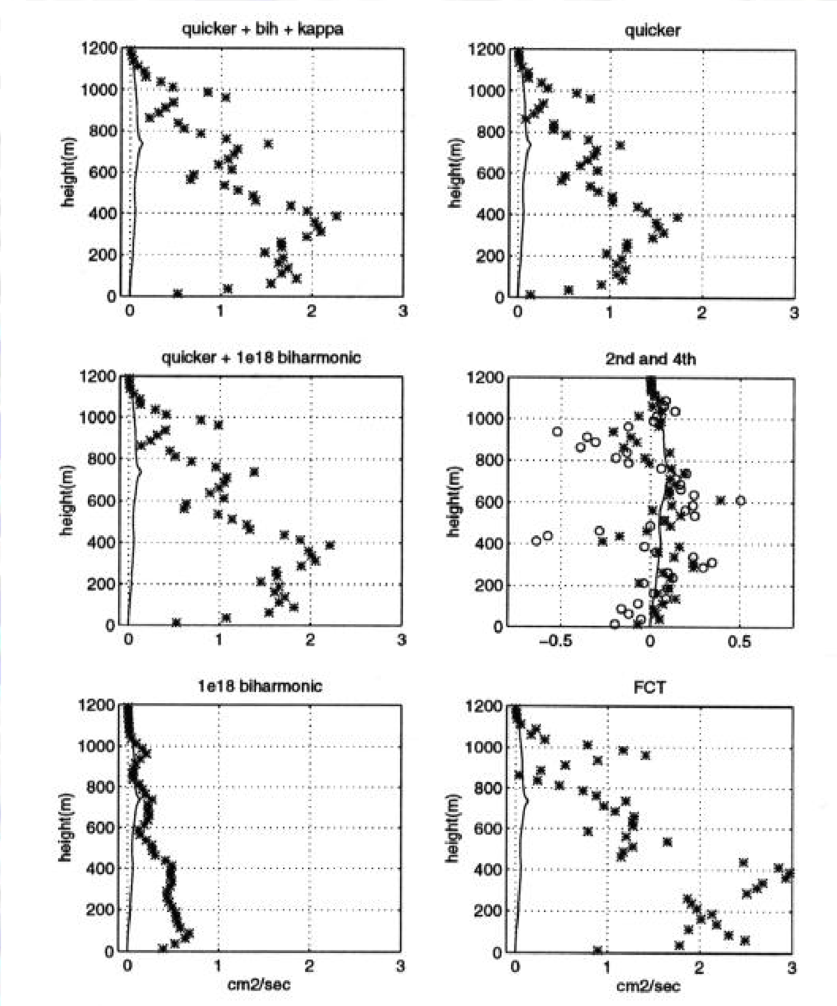

Griffies et al, 2000

Comparison of effective numerical diffusivity with a constant 2.10^{-5} m^2s^{-1}.

Numerical diapycnal mixing

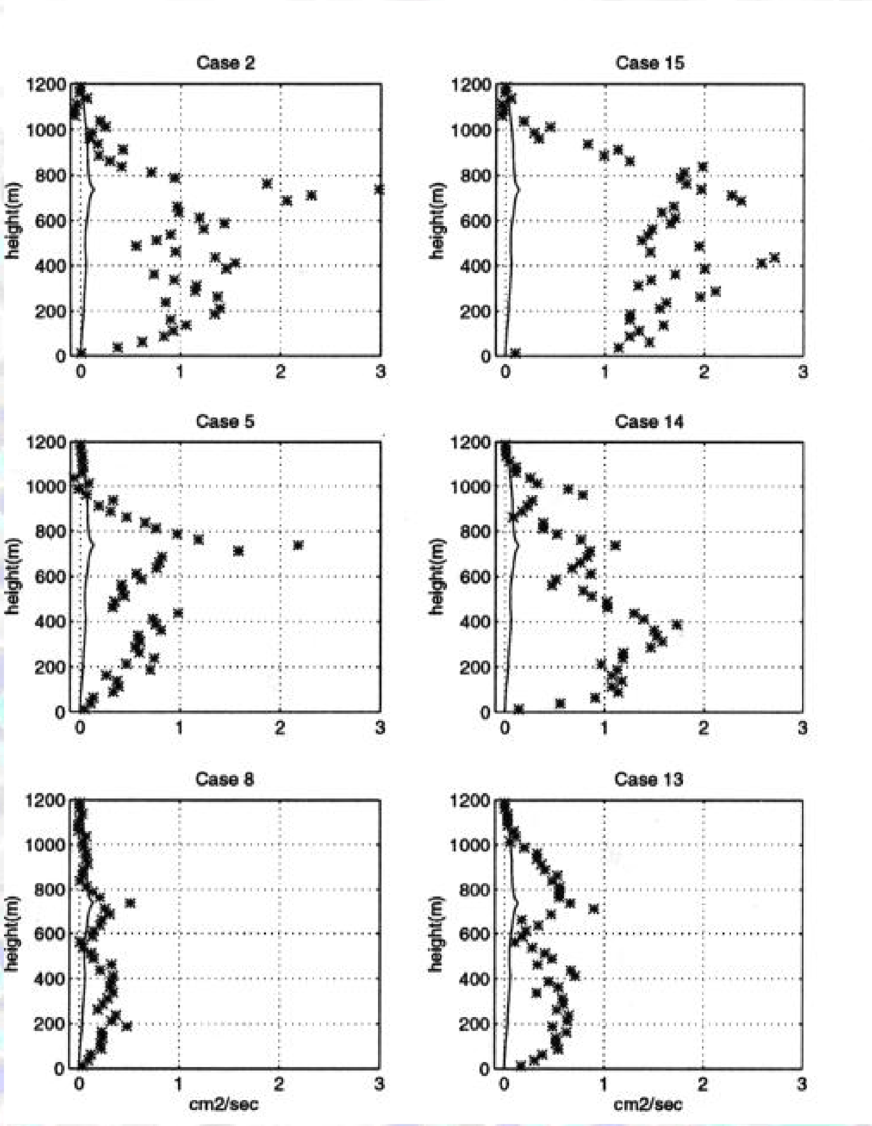

Griffies et al, 2000

Comparison of effective numerical diffusivity with a constant 2.10^{-5} m^2s^{-1}.

Top: 1/3° grid

Middle: 1/6°

Bottom: 1/9°

Quicker advection scheme.

Interior mixing: conclusion

-Surface mixed layer: do we need high resolution or nonloncal schemes? Do we need a mixed layer at all?

-Interior: what is the most appropriate dependency on Ri?

need to take into account tidal and topography enhanced mixing

need to take into account double diffusion.

An accurate parameterization will become more important as we achieve lower amounts of numerical mixing.

2 - Bottom boundary layers and topography

2.a : Bottom boundary layer parameterizations

Bottom boundary layers

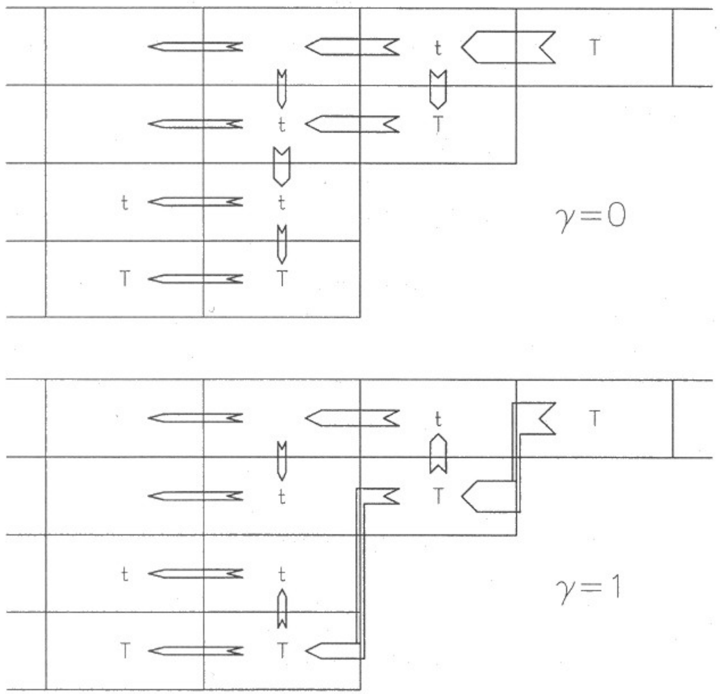

FIG. 2. Schematic representation of barotropic downslope transports at topographic steps for the two extreme values of γ. The thickness of the arrows is proportional to the volume fluxes. For intermediate values of γ a linear superposition of the two patterns

Beckmann and Doscher, 1997.

BBL for tracers:

Create diffusive and/or advective tracer fluxes between bottom cells, conditionally (depending on bottom density).

Bottom boundary layer on momentum?

2 - Bottom boundary layers and topography

In MERSEA 1 models:

No BBL for PSY2, MFS

Gordon *et al* BBL for FOAM.

-modify the bathymetry (?)

-Modified convection scheme of Roether et al.

Bottom boundary layers

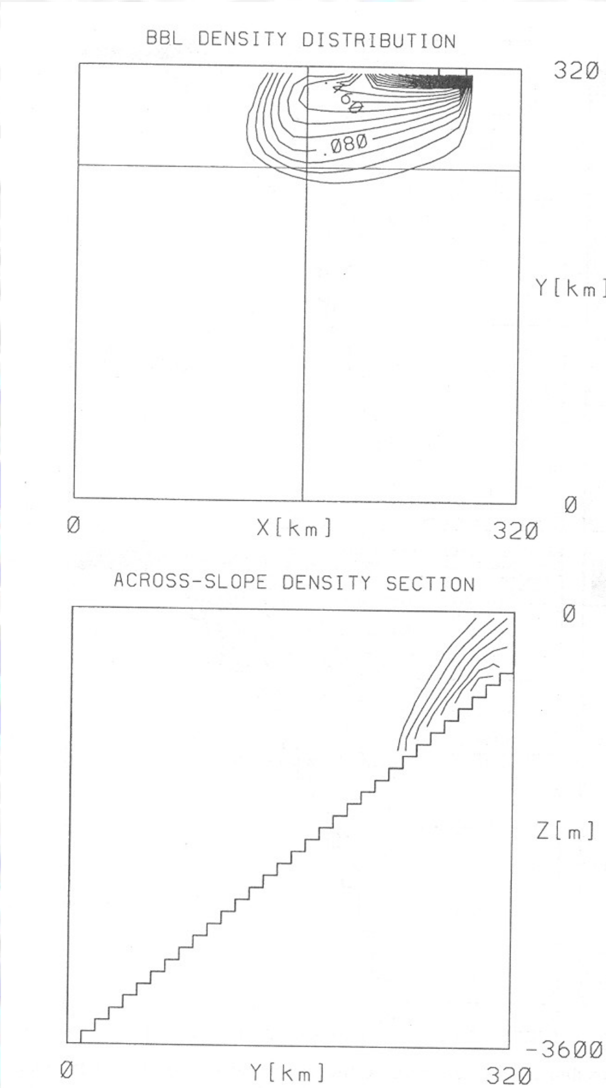

IG. 4a. Results after 50 days for the three-dimensional standard (no BBL M

Flow of dense water down a slope.

Without BBL (left)

With BBL (right)

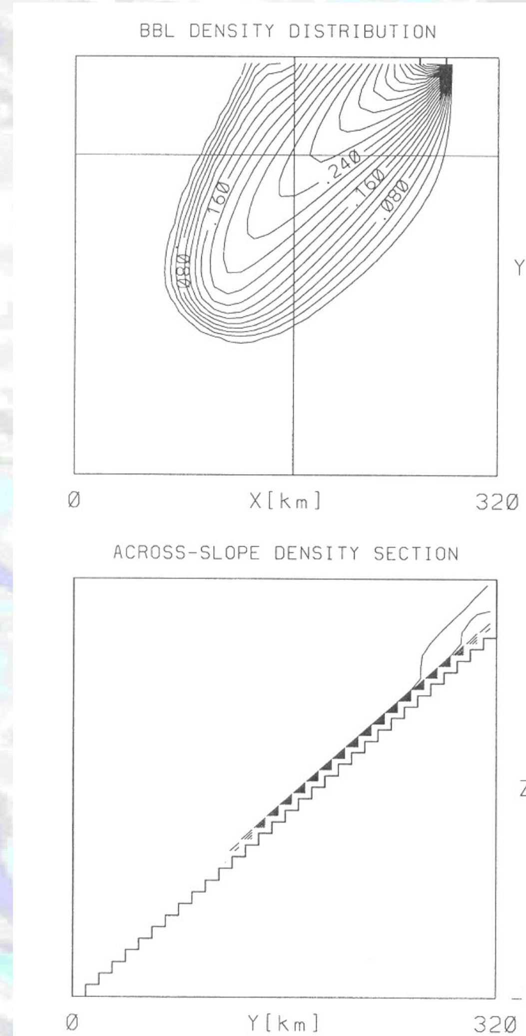

FIG. 4c. As in Fig. 4a but for a coupled

Dense water downstream of Denmark Strait.

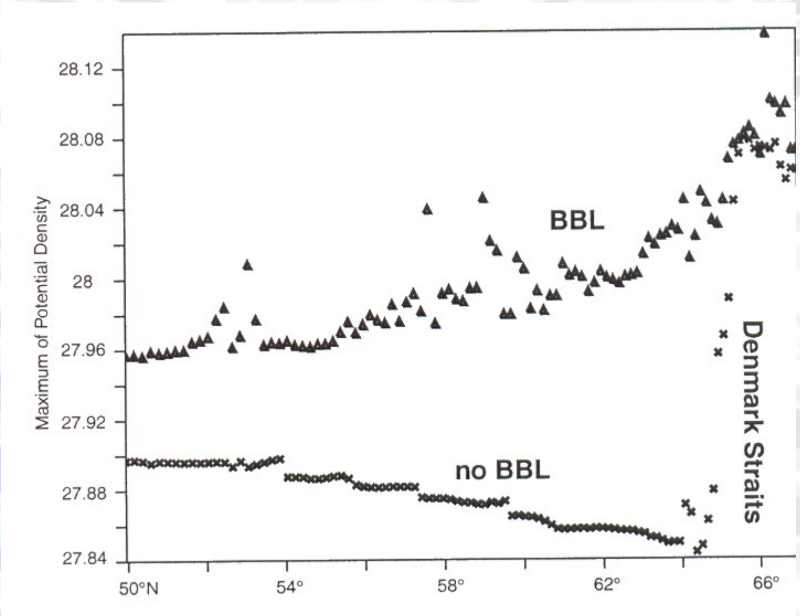

Figure 2. Zonal maximum (between 55°W and 25°W) of potentia density σ_0 at the bottom as a function of latitude south o

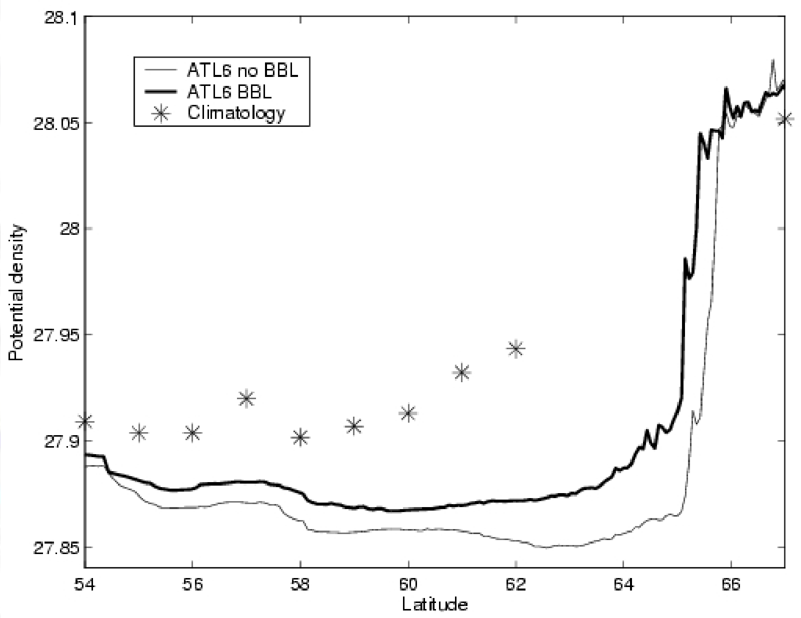

Test in the FLAME 1/3° model.
Dengg et al, 1999.

Test in the ATL6 1/6° model.
De Miranda and Molines, 2002

BBL and overturning

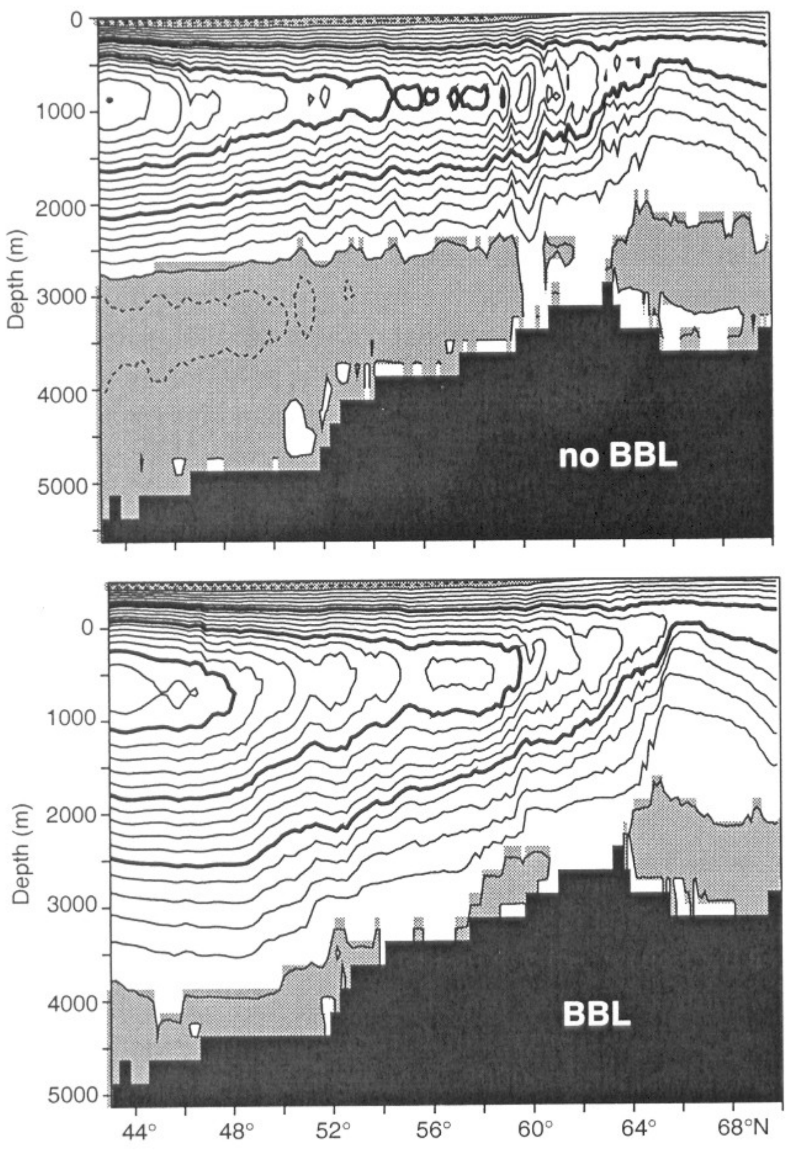

S and T profiles off Portugal in various models

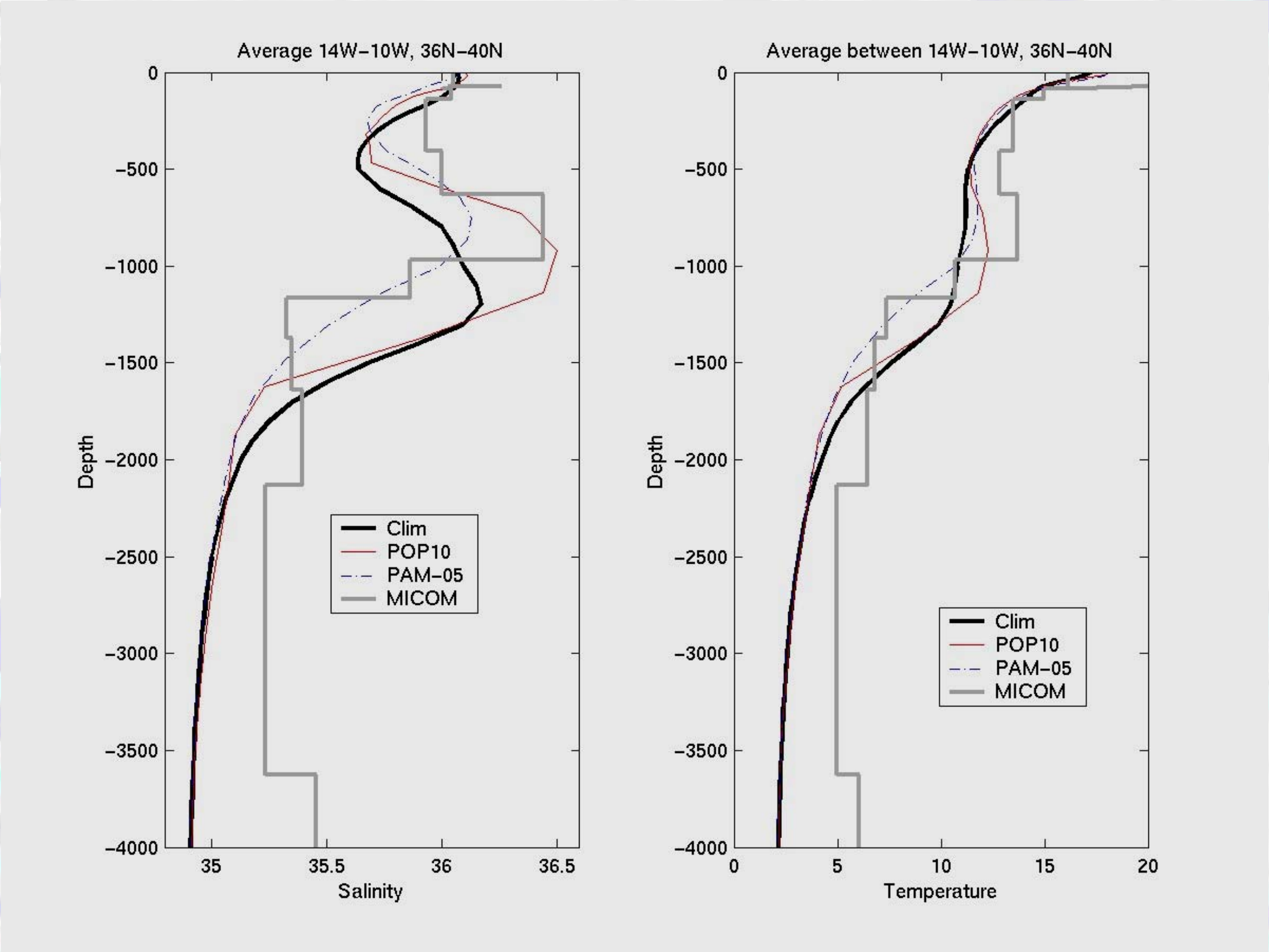

Spreading of Med water – Gulf of Cadiz

Maximum salinity
After 55-60 days

Model: sub-domain of PSY2 (MERCATOR), no Assimilation.
- Centered+upstream advection,
- biharmonic lateral mixing,
- TKE

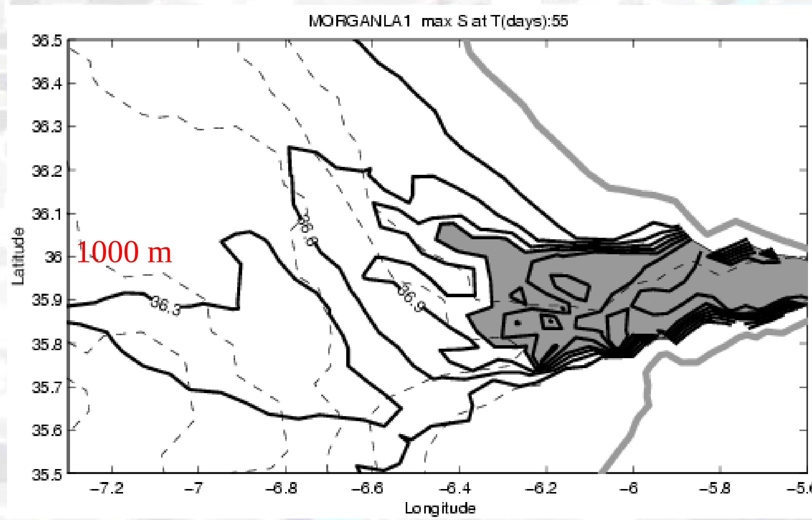

Observations: Johnson et al, 1999.
Grey area : 50% of Med water content,
S > 37.15 PSU.

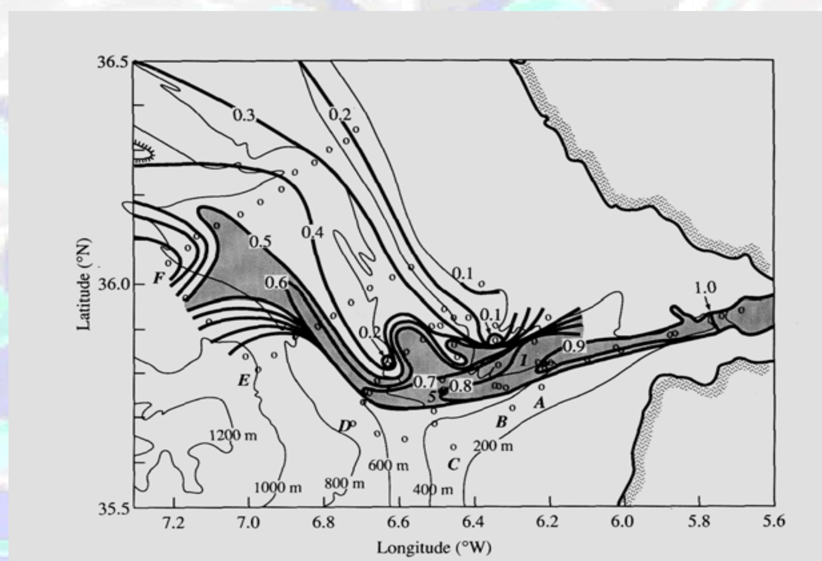

60 days sensitivity studies with PAM -limited area

Observations: *Johnson et al, 1999.*
Grey: 50% Med water,
S > 37.15 PSU.

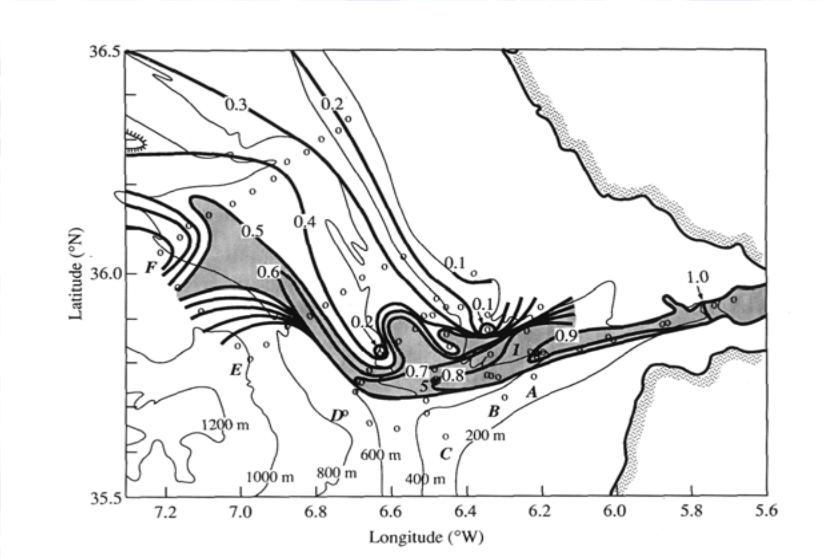

Test model: Bottom boundary
layer (left)
large bottom friction (right)

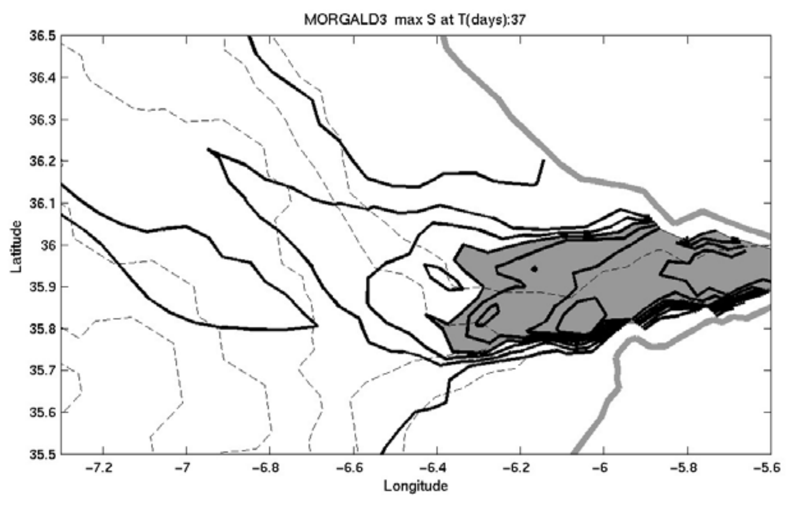

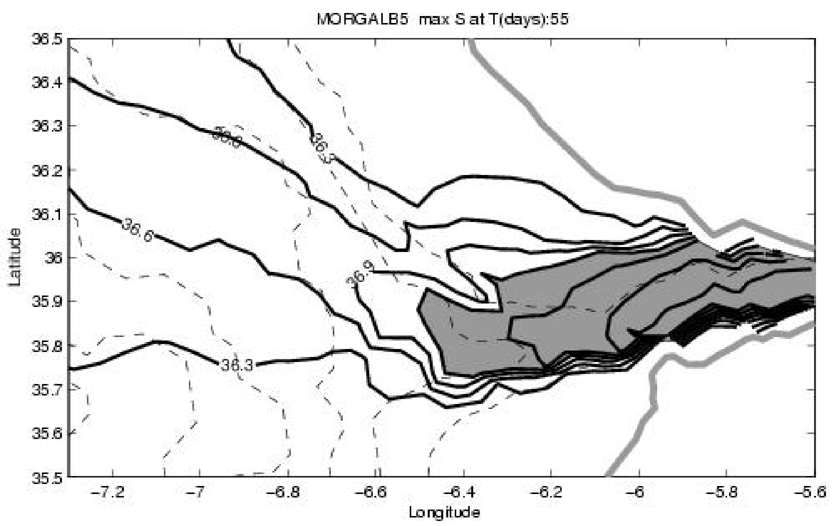

BBL: conclusions

Killworth (‘Aha Hulikoa, 2003)

- A good BBL must work everywhere

-A parameterization is no substitute for resolution: easier to achieve in sigma models (but pressure gradient errors).

- Are we able, by looking at model results, to demonstrate the performance of simple vs. elaborate BBLs? Are parameterizations/topography/numerics interactions obscuring the issue?

-Potential use of CFCs for validation.

2 - Bottom boundary layers and topography

2.b : Topography subgrid scale

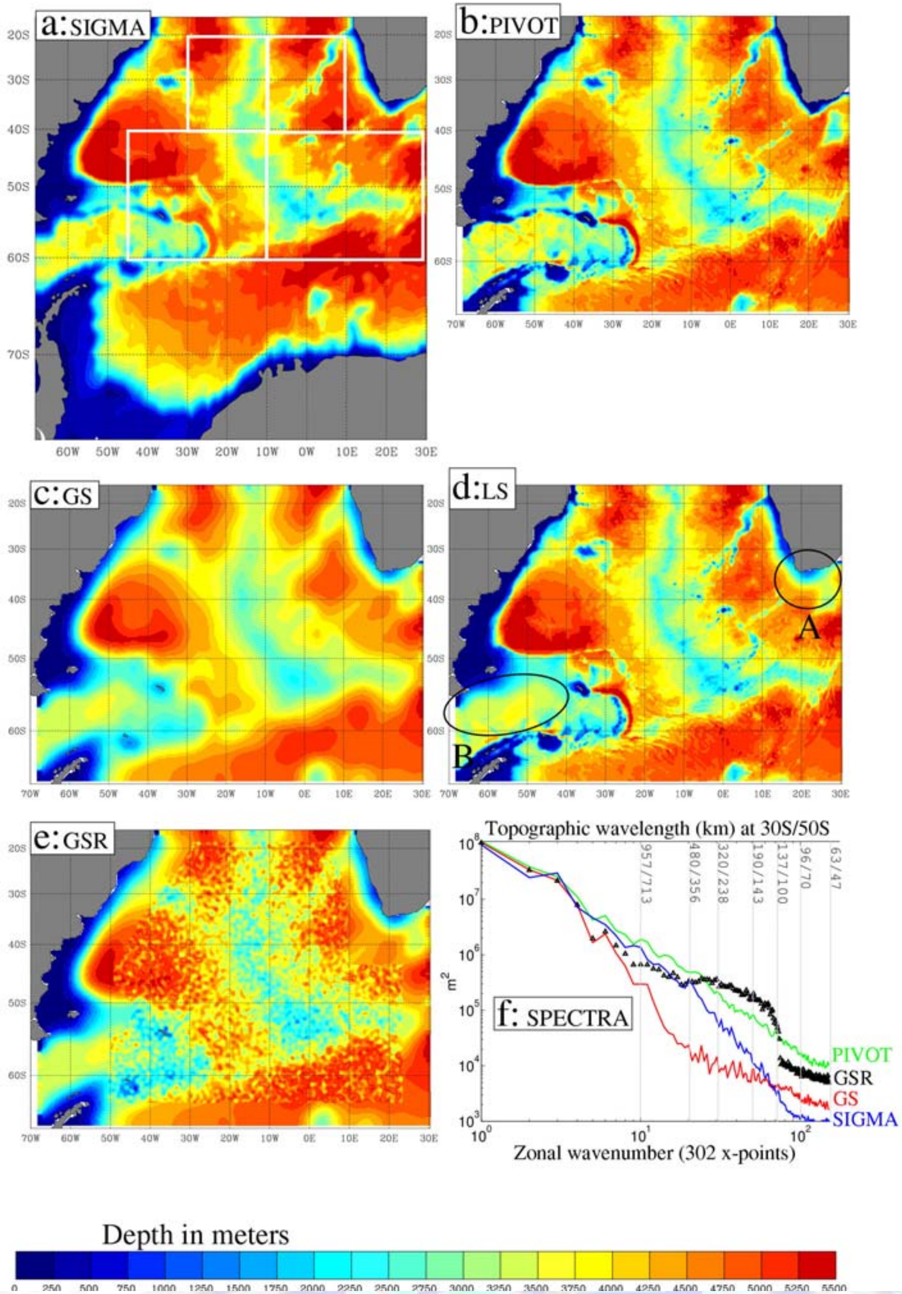

Subgrid scale topographic roughness

Comparison of a sigma model, and level models with various degrees of topographic smoothing (Penduff et al, J.P.O., 2002).

Subgrid scale topographic roughness

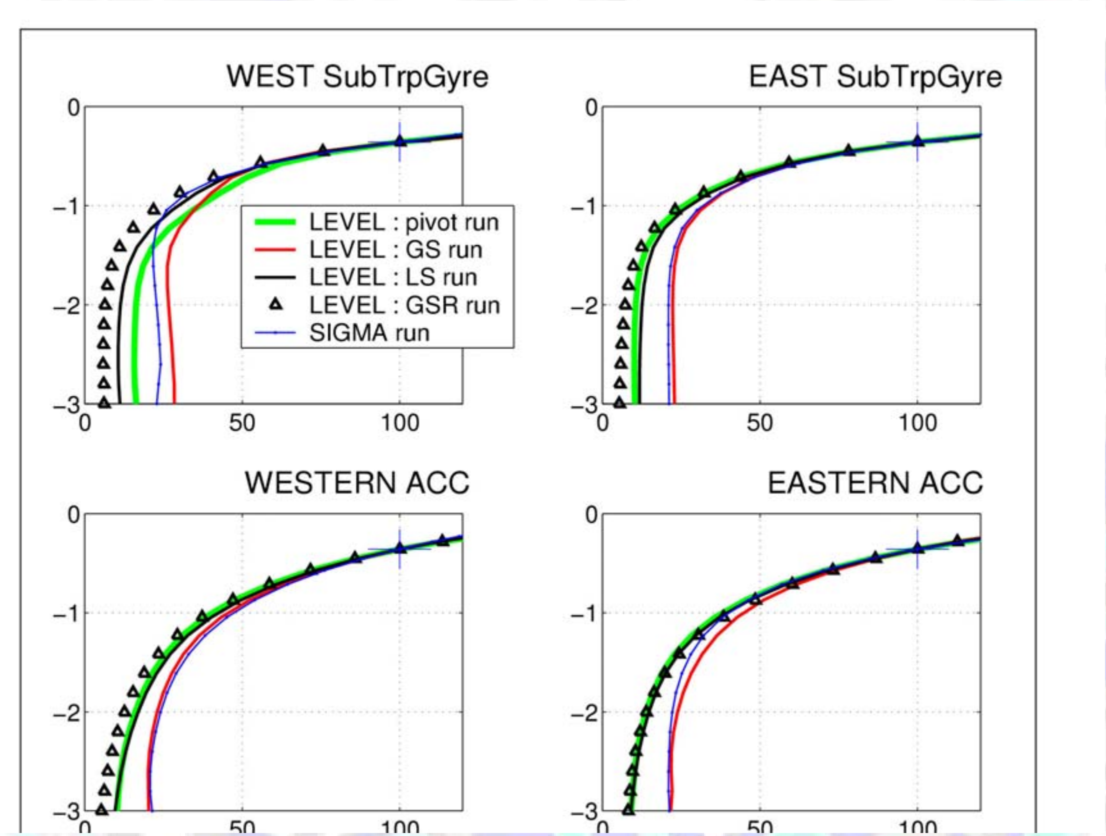

Eddy kinetic energy is too surface – intensified in level models with unfiltered topography.

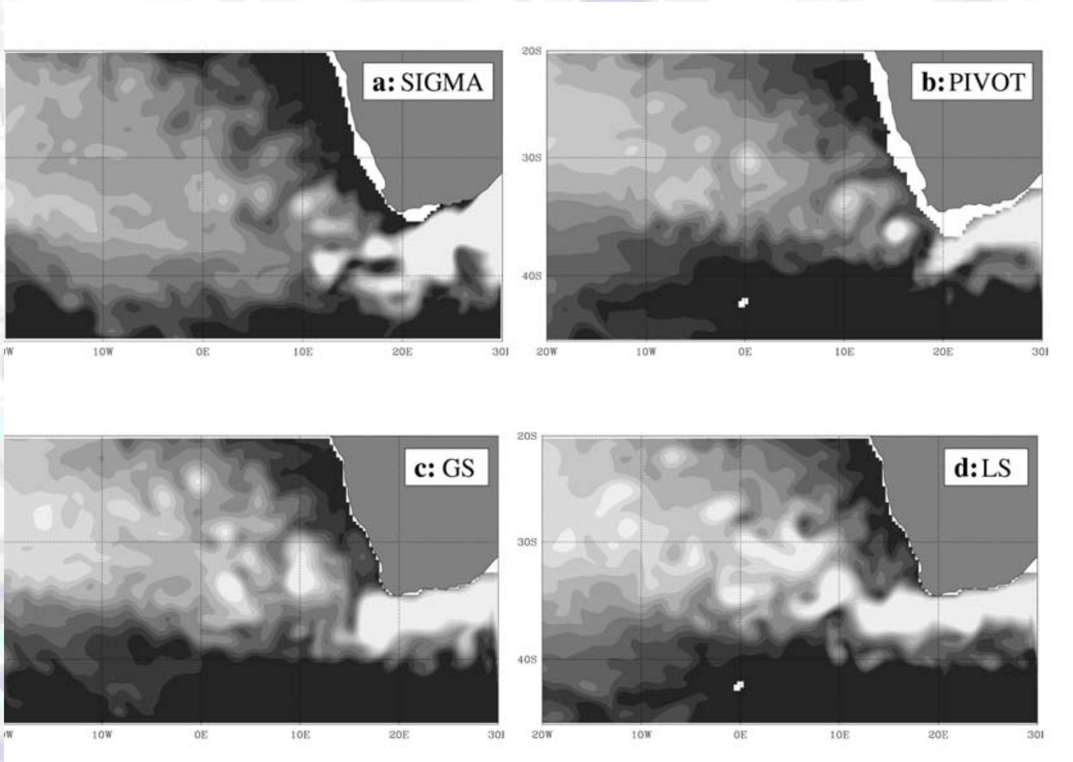

Subgrid scale topographic roughness

It decreases the eddy kinetic energy at depths and renders the flow more baroclinic,

Unfiltered staircase topography already does this (even too much) in z-models.

2 - Bottom friction

- Essential mechanism in QG models: energy sink for the barotropic mode.

- Baroclinic instability is sensitive to bottom friction

Bottom friction

Rivière et al, JPO, 2004: bottom friction changes the properties of a baroclinically unstable jet

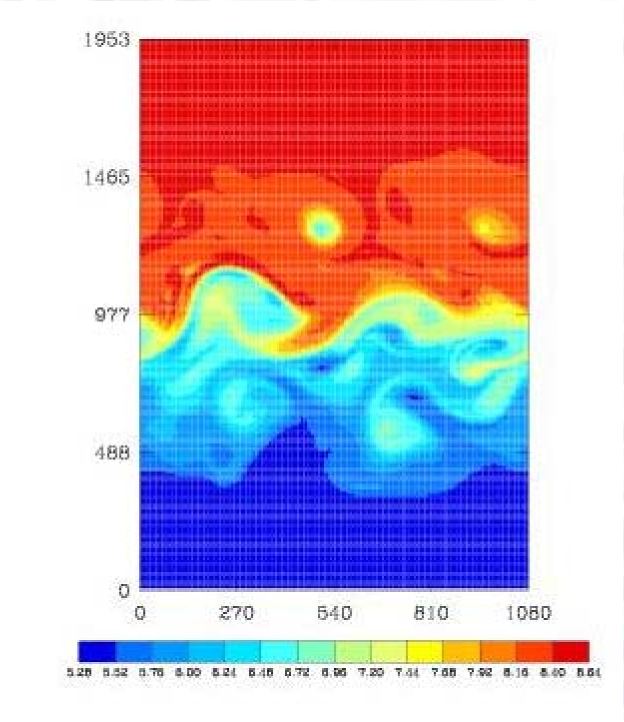

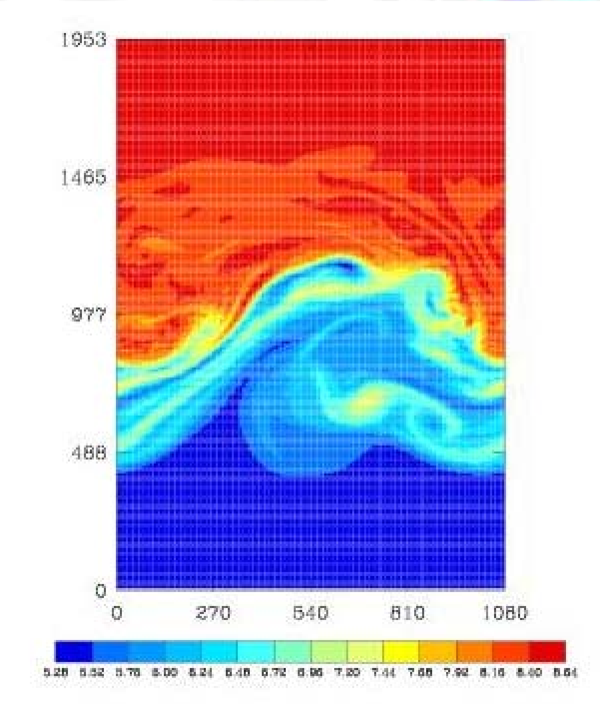

High bottom friction (100 days) Smaller wavelength, more isolated eddies.

Low bottom friction (800 days) long wavelength, barotropic flow.

2 - Bottom friction

QG models have linear friction with decay time of about 100 days in a bottom layer of typical depth 3000m

- A P.E. model with linear or quadratic friction compares well with a QG model when the decay time is estimated for the total ocean depth.

- What about lateral friction on the bottom in a z-coordinate model?

3. Lateral mixing of tracers

Lateral mixing is along isopycnals

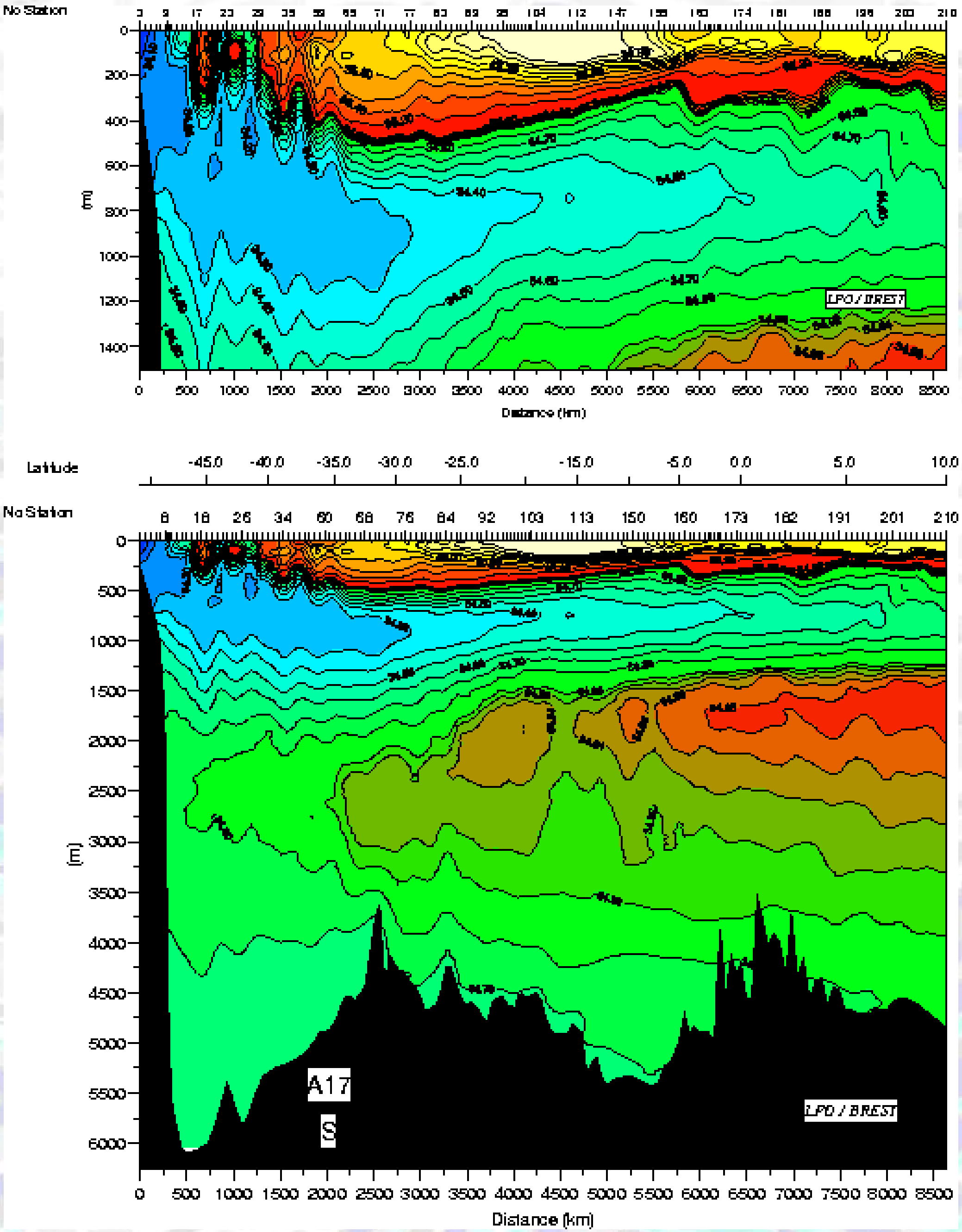

Isopycnal mixing of tracers

Tracers (T, S anomalies, oxygen, freons…) are mixed along isopycnals at the large scale

Isopycnal rotation of tensor (3D)

Isopycnal rotation of the tensor (Redi, 1982)

$$\kappa^* = \frac{\kappa_h}{\rho_x^2 + \rho_y^2 + \rho_z^2},$$

$$\mathbf{K}^g = \kappa^* \begin{bmatrix} \rho_z^2 + \rho_y^2 + \epsilon\rho_x^2 & (\epsilon - 1)\rho_x\rho_y & (\epsilon - 1)\rho_x\rho_z \\ (\epsilon - 1)\rho_x\rho_y & \rho_z^2 + \rho_x^2 + \epsilon\rho_y^2 & (\epsilon - 1)\rho_y\rho_z \\ (\epsilon - 1)\rho_x\rho_z & (\epsilon - 1)\rho_y\rho_z & \rho_x^2 + \rho_y^2 + \epsilon\rho_z^2 \end{bmatrix}.$$

Isopycnal mixing of tracers

Observations (NATRE, Ledwell et al, 1998):

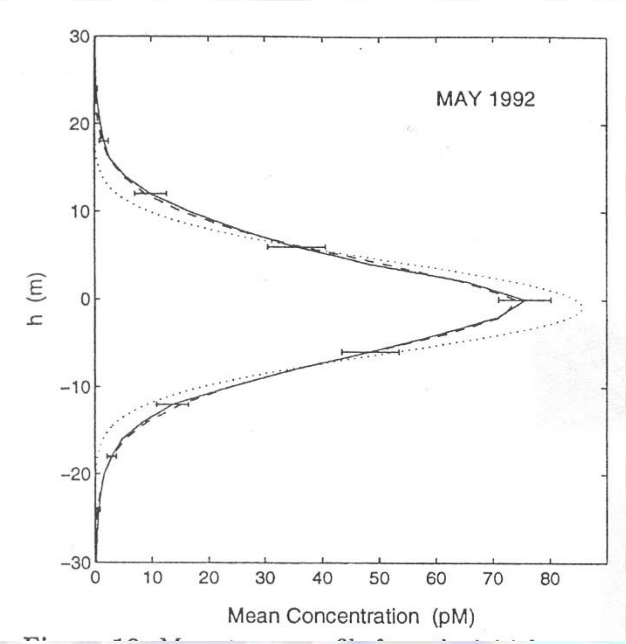

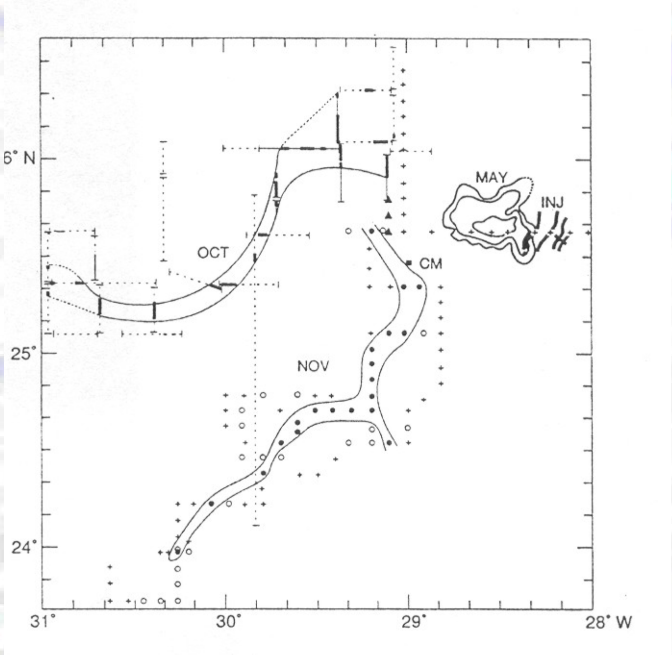

Evolution of the tracer distribution in the vertical (diffusion)

Evolution along isopycnals: eddy stirring.

Isopycnal mixing of tracers

Observations:

- mixing is along isopycnals down to the km scale;
- mixing is smaller at small scales: 2 m^2/s at scales de 1-30 km, up to 1000 m^2/s at scales larger than 300 km
- Mesoscale eddies stir the tracer into elongated filaments

Mersea 1 lateral parameterizations

	PSY2	FOAM	MSF1	MFS2
Diffusivity	biharm	laplacian	biharm	biharm
ν_T	$3\ 10^9$	$100\ m^2s^{-1}$	$1.5\ 10^{10}$	3.10^9
orientation	hor	Iso+backg.	hor	hor
Viscosity				
$\nu_m\ (m^4s^{-1})$	$9\ 10^9$	$2.6\ 10^9$	$5.\ 10^9$	5.10^9
$\nu_m\ (m^2s^{-1})$		30		

Laplacian/ biharmonic

$\partial T/\partial t = \kappa_l \, \partial^2 T/ \partial x^2$ wavelength λ, decay time $\tau = (\lambda/2\pi)^2/ \kappa_l$

$\partial T/\partial t = \kappa_b \, \partial^2 T/ \partial x^4$ wavelength λ, decay time $\tau = (\lambda/2\pi)^4/ \kappa_b$

Cut-off wavelength ($2\delta x$)

FOAM (2*12 km, κ_l =100) τ= 1.6 days

MFS (2*6 km, κ_b = 3. 10^9) τ= 1h

Well resolved wavelength

FOAM (120 km, κ_l =100) τ= 169 days

MFS (120 km, κ_b = 3. 10^9) τ= 8000 days

Isopycnal mixing of tracers

Comparison with the CLIPPER 1/6° Atlantic model (J.M. Molines, A. de Miranda, B. Barnier)

-ATL6-V5, 8 years spin up, biharmonic coefficient with δx^3 dependency

- ATL6-10, 8 year spin-up with isopycnal laplacian, coefficient 200m²/s

Biharmonic/isopycnal laplacian

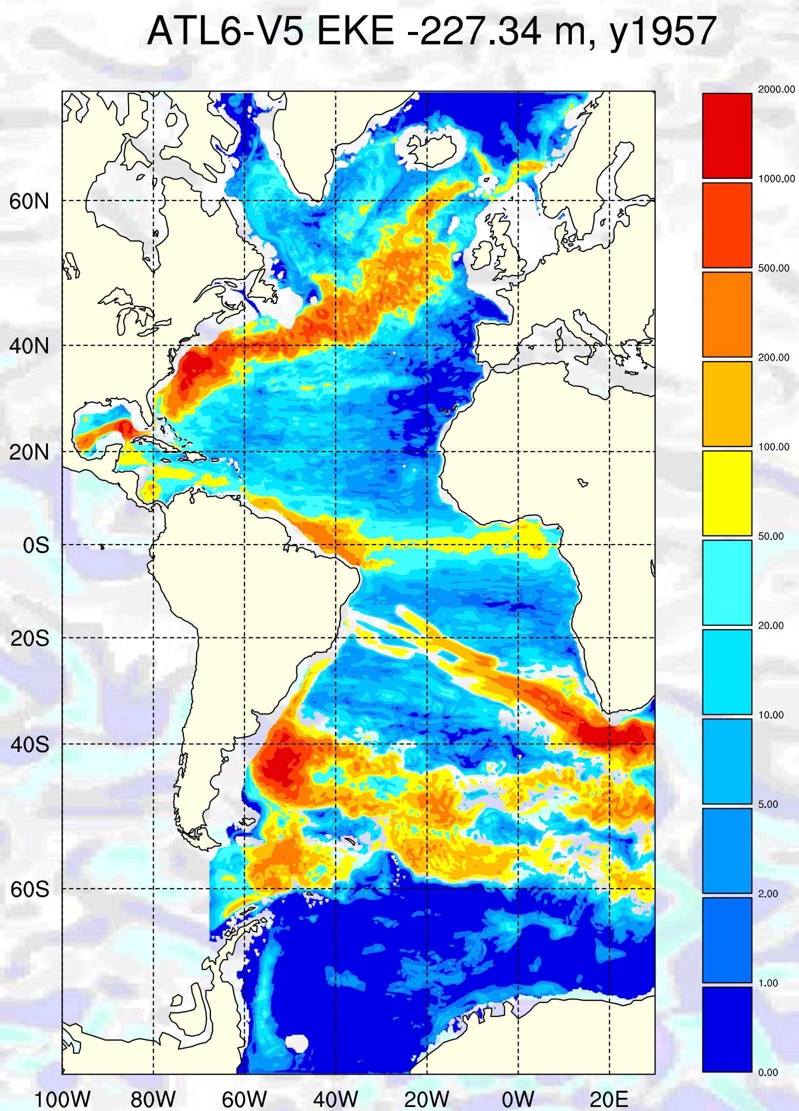

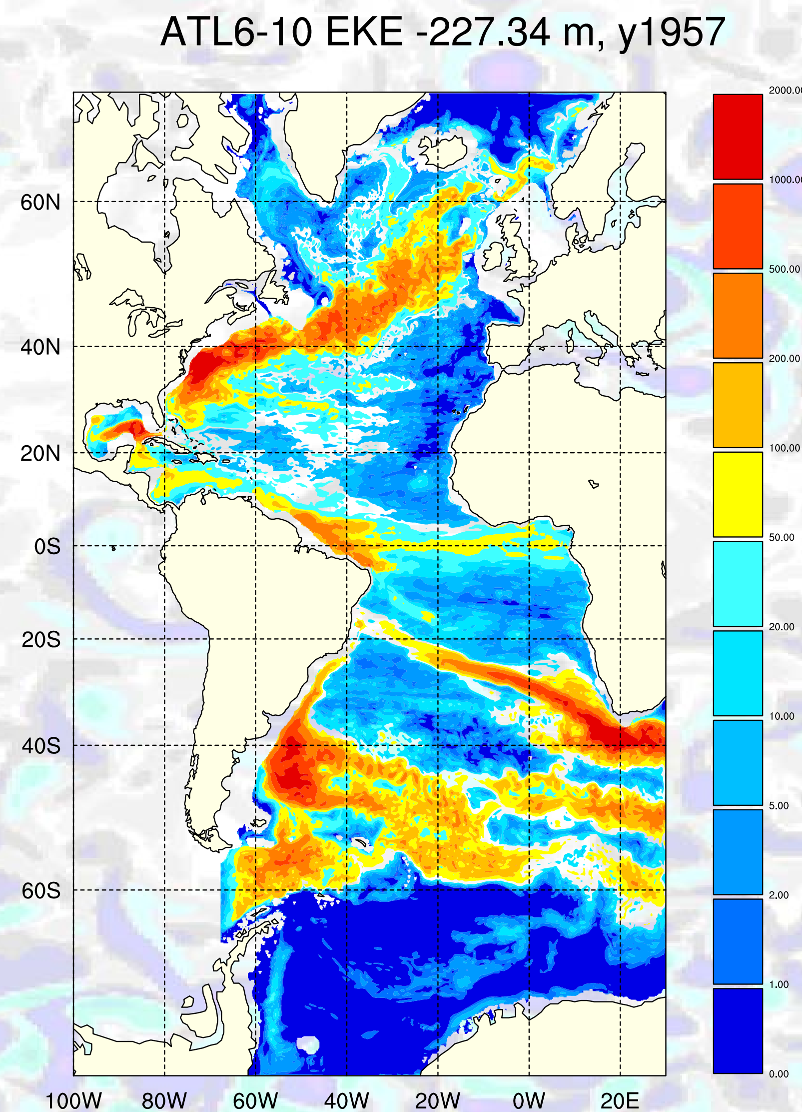

Biharmonic/isopycnal Laplacian

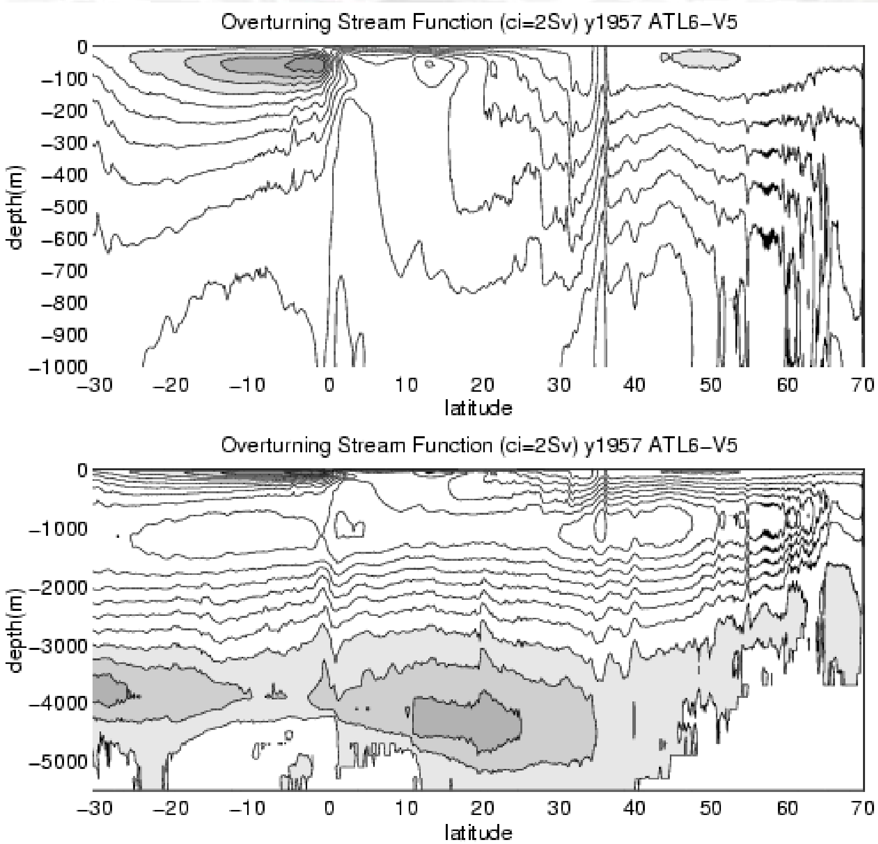

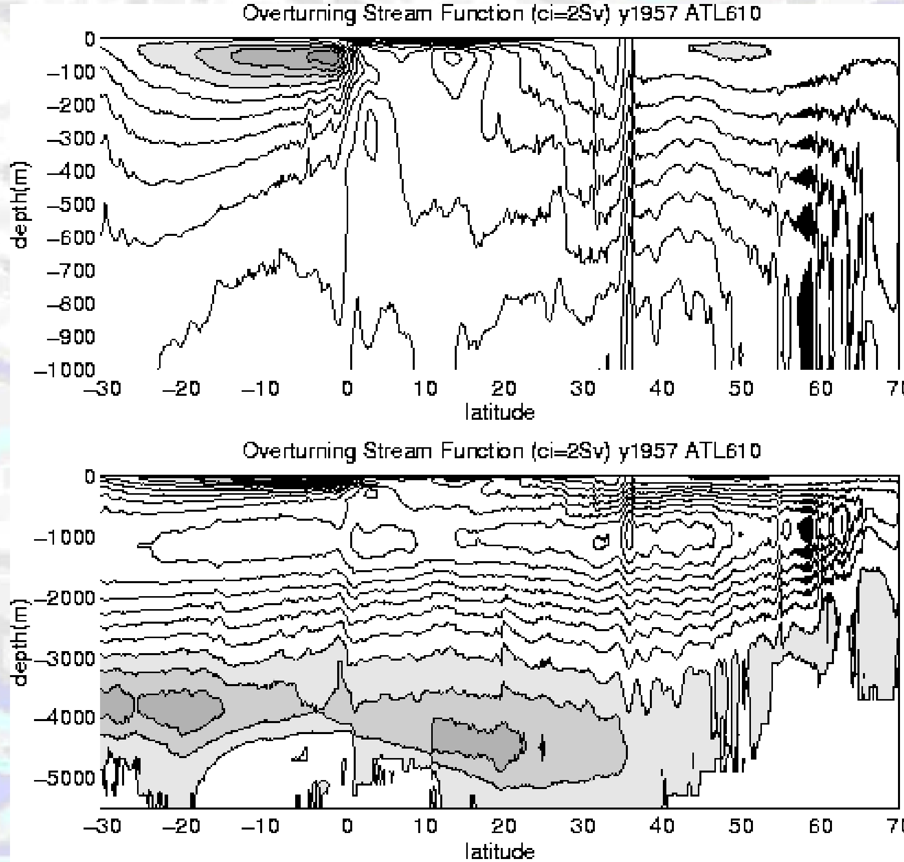

Overturning is larger than 2 Sv with isopycnal laplacian

Biharmonic/isopycnal Laplacian

48°N section

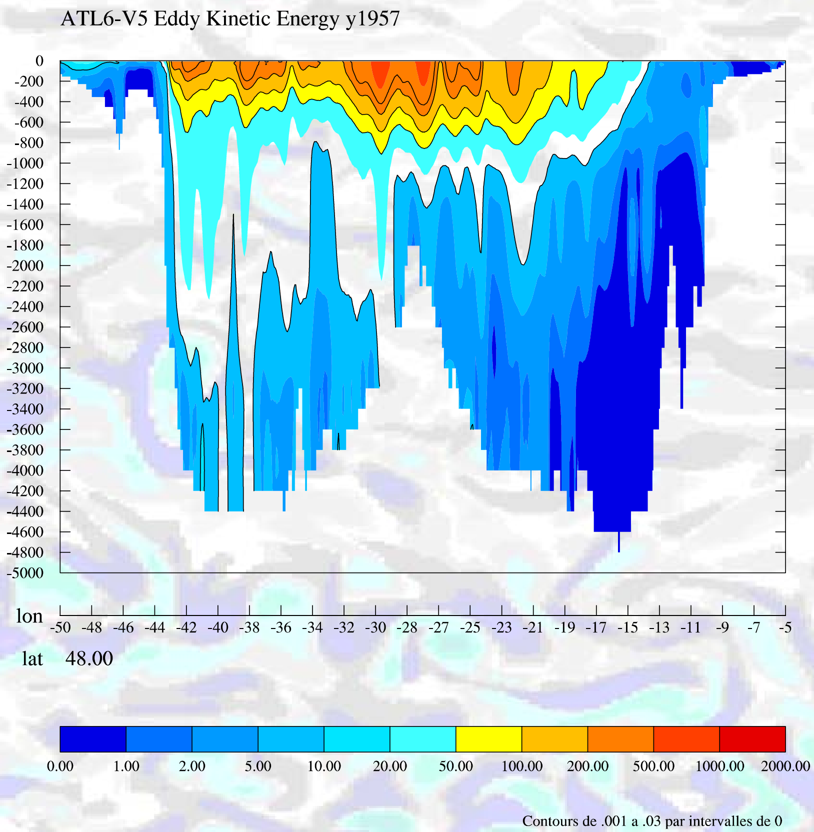

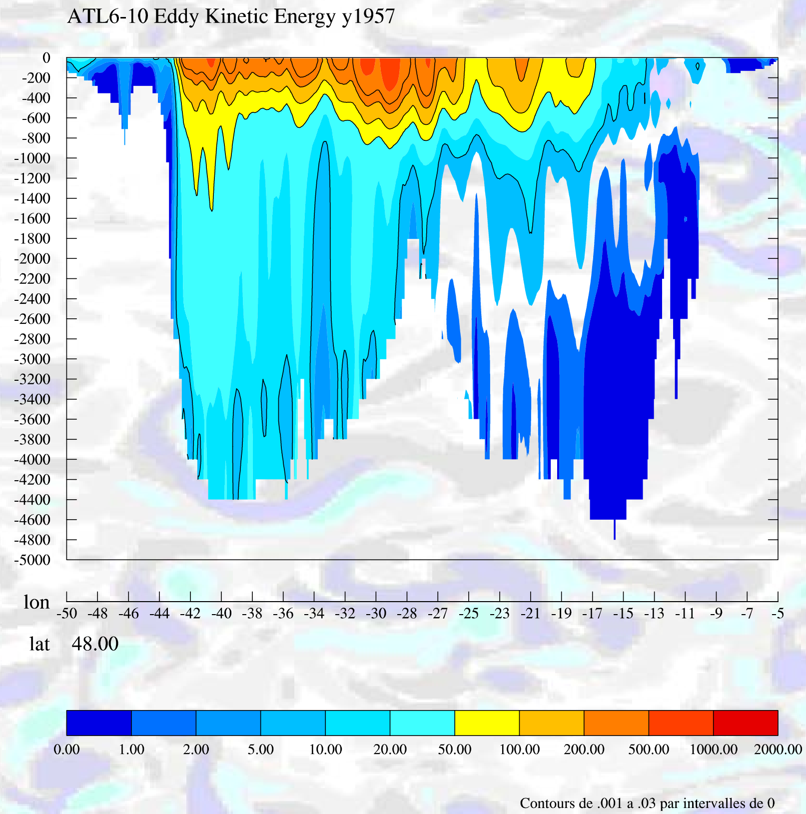

Better penetration of the eddy kinetic energy at depth

Mersea 1 lateral parameterizations

	PSY2	FOAM	MSF1	MFS2
Diffusivity	biharm	laplacian	biharm	biharm
ν_T	$3\ 10^9$	$100\ m^2s^{-1}$	$1.5\ 10^{10}$	3.10^9
orientation	hor	Iso+backg.	hor	hor
Viscosity				
$\nu_m\ (m^4s^{-1})$	$9\ 10^9$	$2.6\ 10^9$	$5.\ 10^9$	5.10^9
$\nu_m\ (m^2s^{-1})$		30		

Inhomogeneity of the mesoscale eddy field

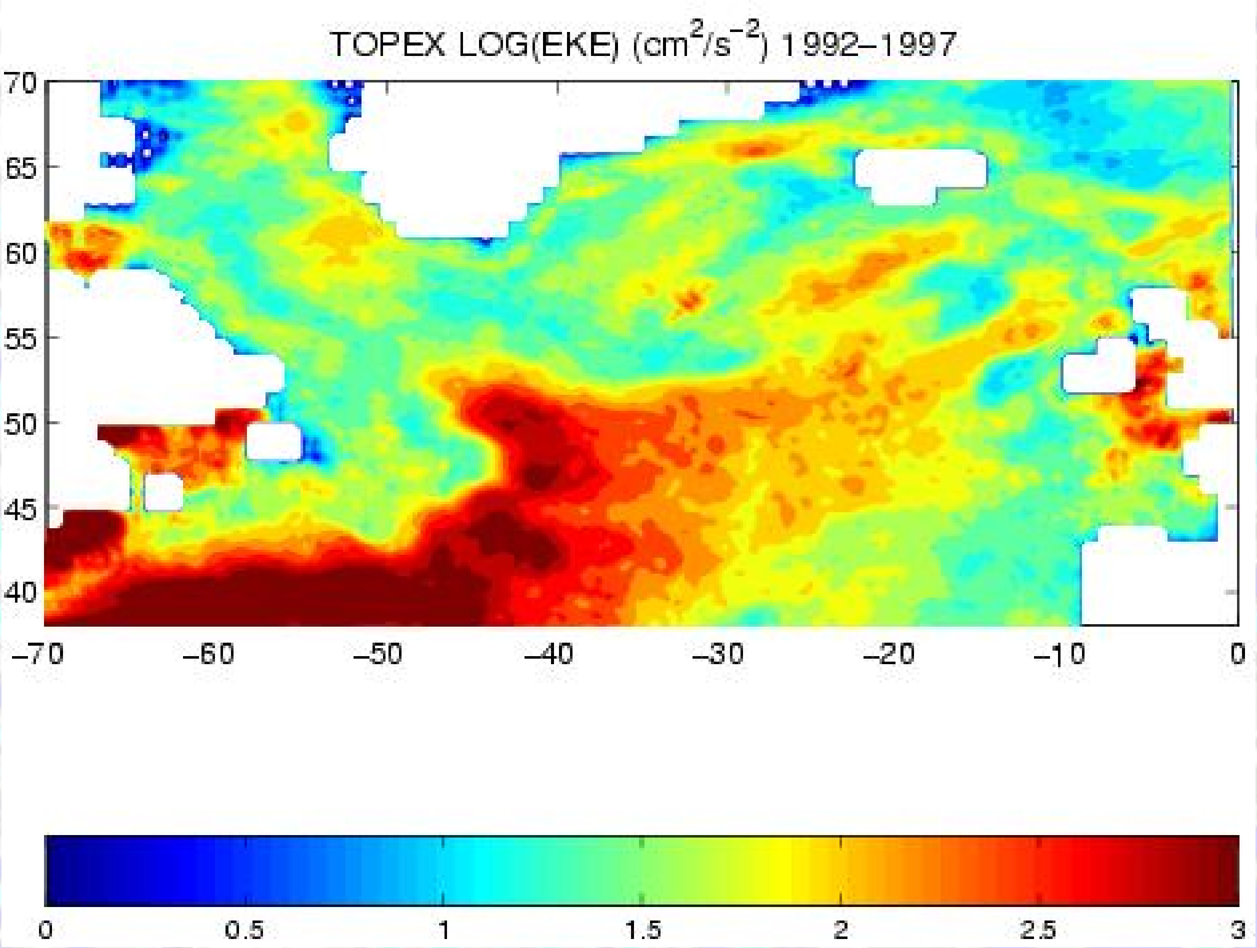

A variable eddy mixing coefficient

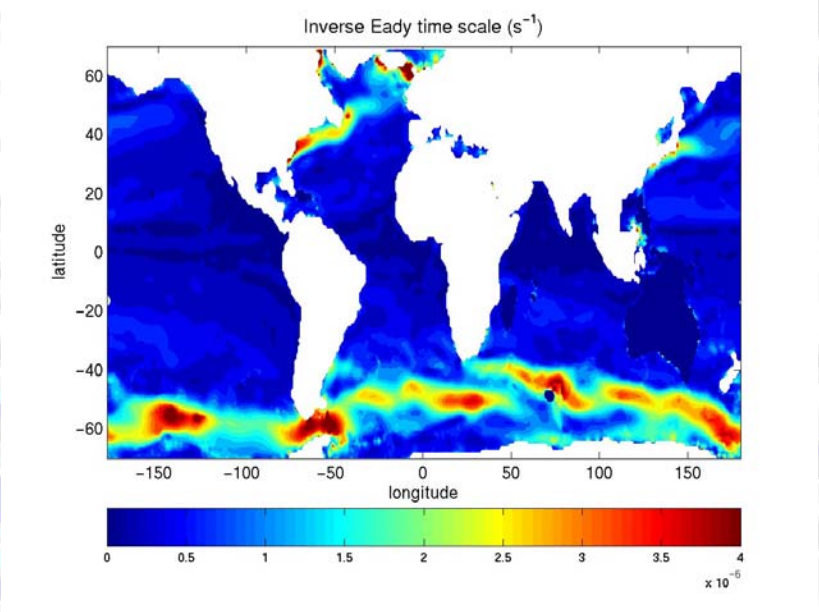

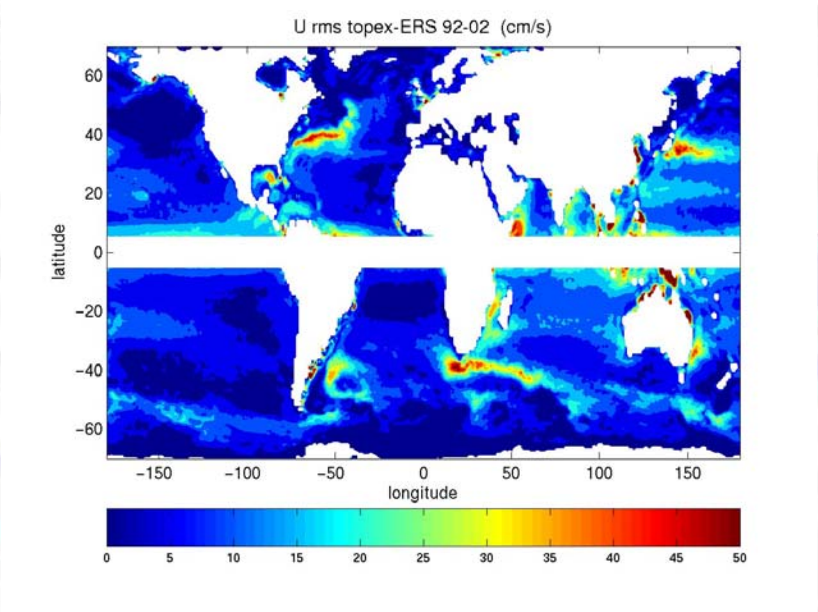

Inverse Eady time scale (growth rate of baroclinic instability):

$I = f\,|\partial U/\partial z|\,/N$

Treguier et al, 1997

Rms geostrophic eddy velocity from TOPEX-ERS satellites (le Traon et al).

Inhomogeneity of mesoscale mixing

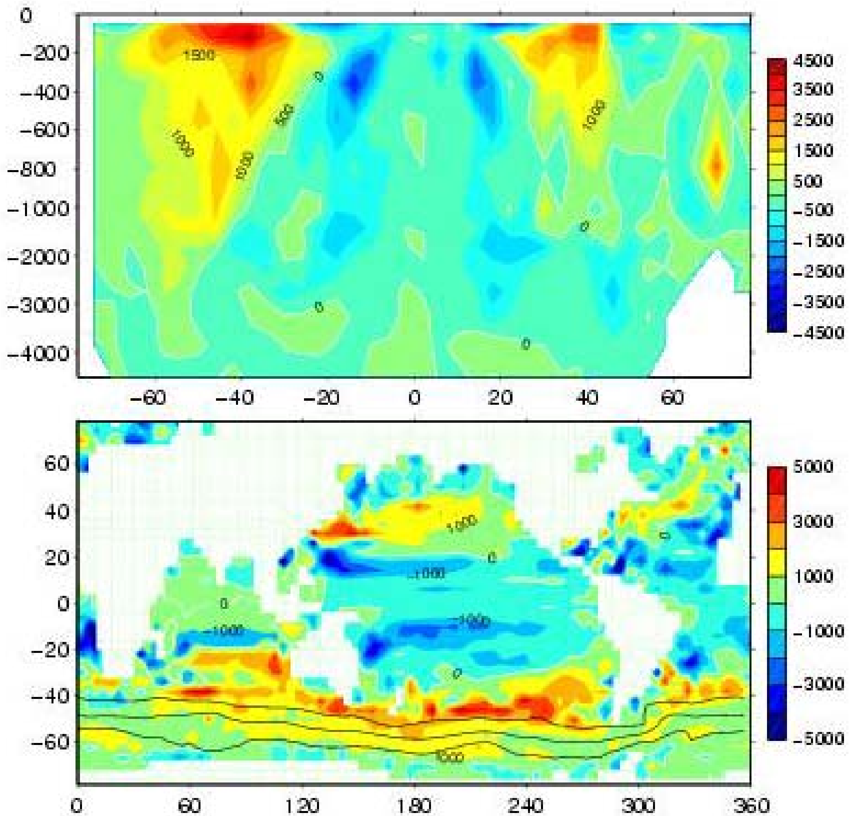

Figure 12: Inferred horizontal eddy diffusivity κ in $m^2\ s^{-1}$: (top) zonal mean and (bottom) vertical mean over the thermocline (0-1200 m). The contour interval is 500 $m^2\ s^{-1}$ in the top panel and 1000 $m^2\ s^{-1}$ in the bottom one. The thick line indicates the zero contour. Also indicated in the bottom panel, the 10, 70 and 130 Sv contours of the barotropic streamfunction.

Mixing coefficients inferred from a coarse resolution model, using an adjoint method and eddy stress formulation.

Ferreira and Marshall, 2004

Vertical structure of isopycnic mixing

Mixing coefficient as a function of depth in an unstable jet in a channel (Treguier, 1999).

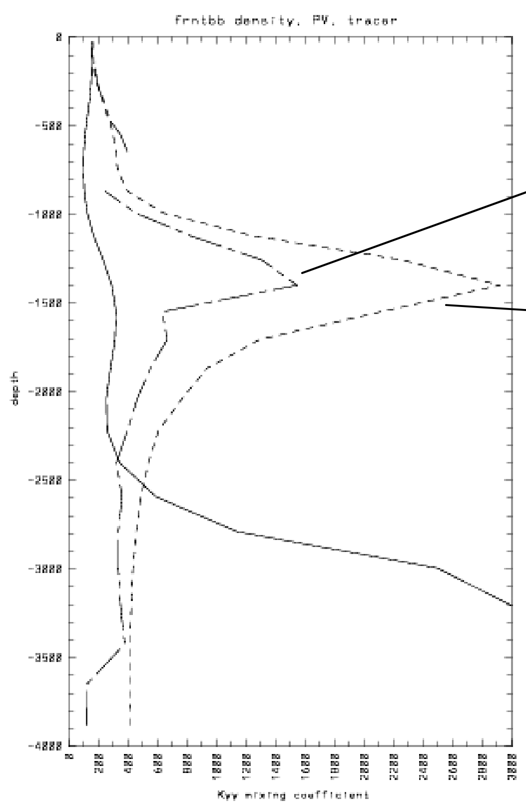

Coefficient for isopycnal mixing of Potential vorticity

Coefficient for isopycnal mixing of a passive tracer

Eke is maximum at the surface

Mixing is maximum below the jet core (steering level).

Vertical structure of isopycnic mixing

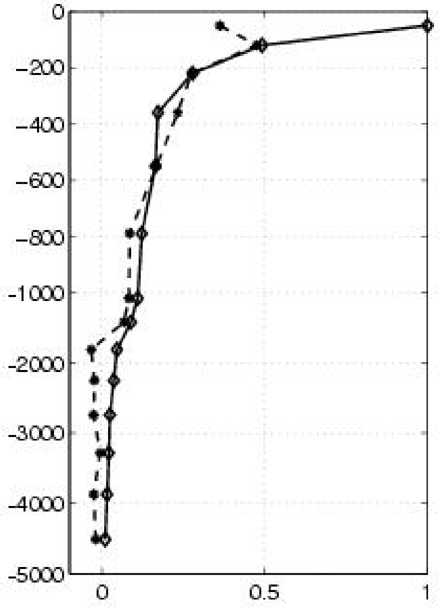

Figure 13: Averaged vertical profile of the inferred eddy diffusivity κ (divided by 6000 $m^2\ s^{-1}$, solid) and of the buoyancy frequency N^2 normalized by its surface value (dashed). The averaging area is extend from 65°S to 30°S and from 30°N to 45°N where the diffusivities are mainly positive.

Mixing coefficient inferred in a coarse resolution model using an adjoint method and an eddy stress formulation (Ferreira and Marshall 2004).

Isopycnal mixing of tracers

Mixing by mesoscale eddies in spatially variable

Mixing by mesoscale eddies depends on depth.

What about the submesoscale?

Inhomogeneity of the submesoscale eddy field

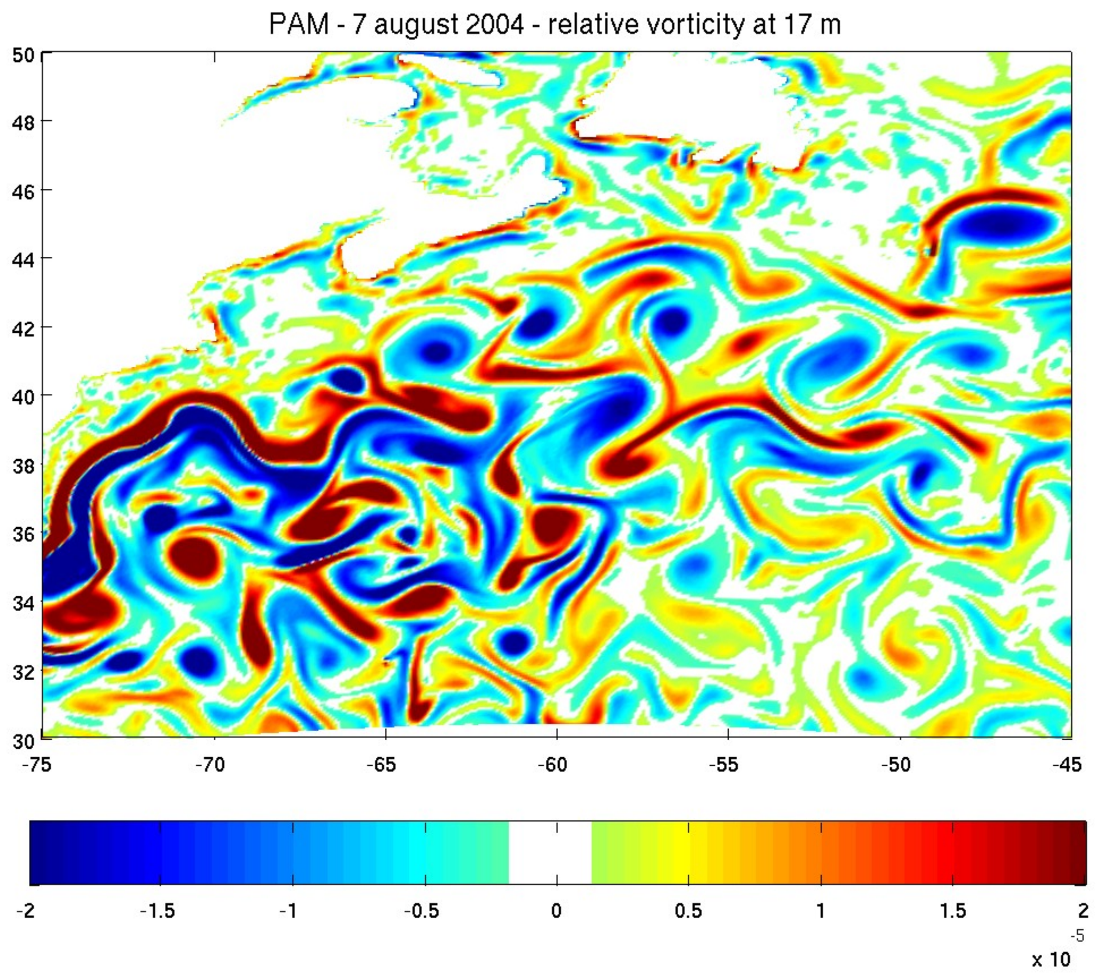

(PAM… PSY)

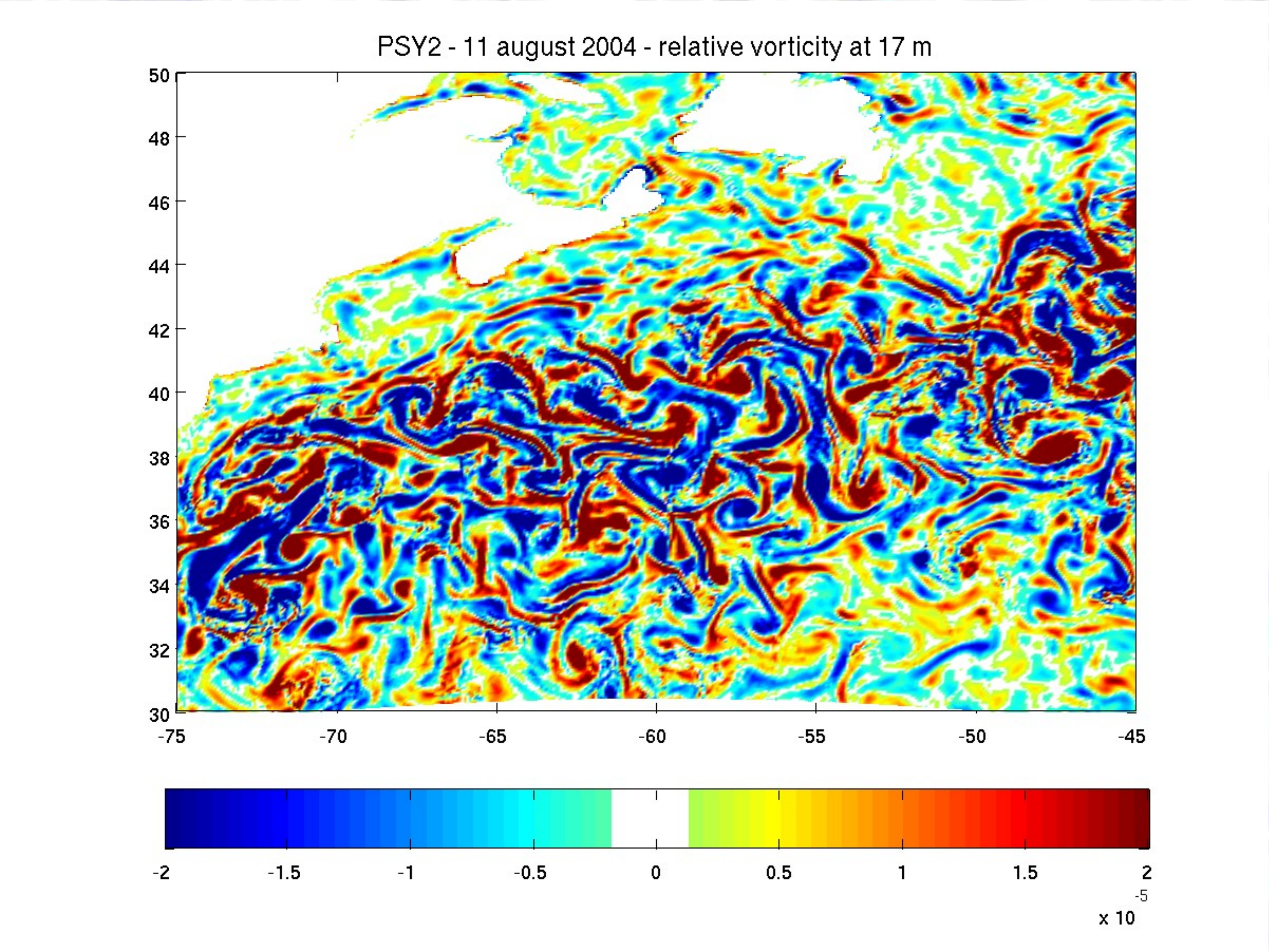

PSY2 - 11 august 2004 - relative vorticity at 17 m
50
48
46
44
42
40
38
36
34
32
30
-75
-70
-65
-60
-55
-50
-45
-2
-1.5
-1
-0.5
0
0.5
1
1.5
2
x 10
-5

Hycom

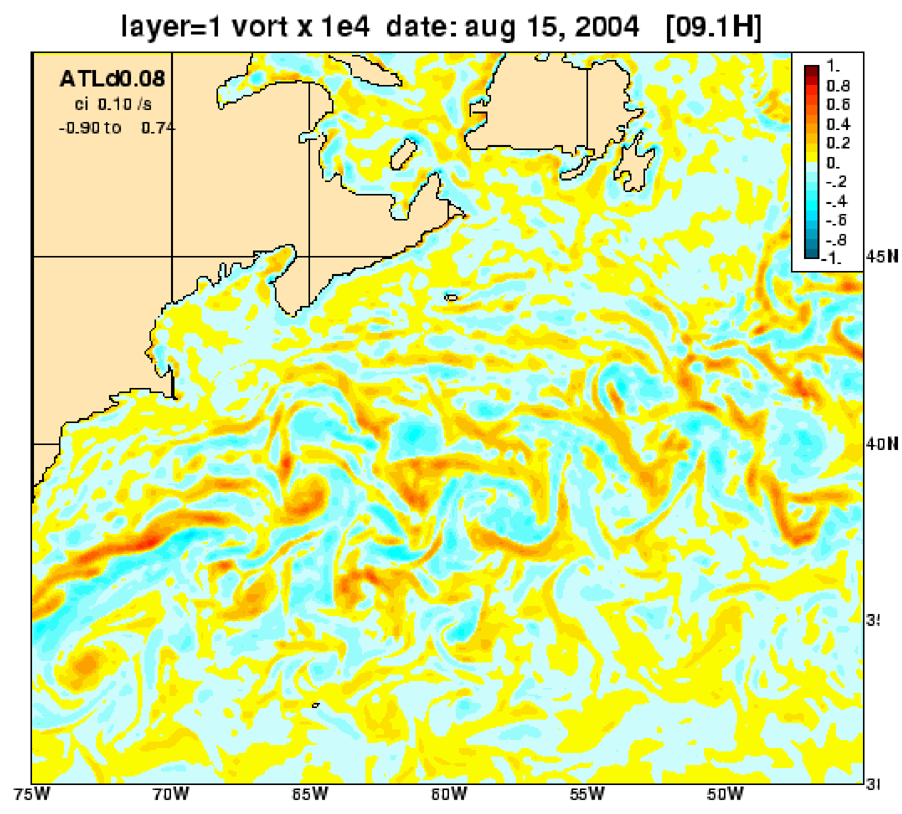
layer=1 vort x 1e4 date: aug 15, 2004 [09.1H]
ATLd0.08
ci 0.10 /s
-0.90 to 0.74
1.
0.8
0.6
0.4
0.2
0.
-.2
-.4
-.6
-.8
-1.
45N
40N
75W
70W
65W
60W
55W
50W

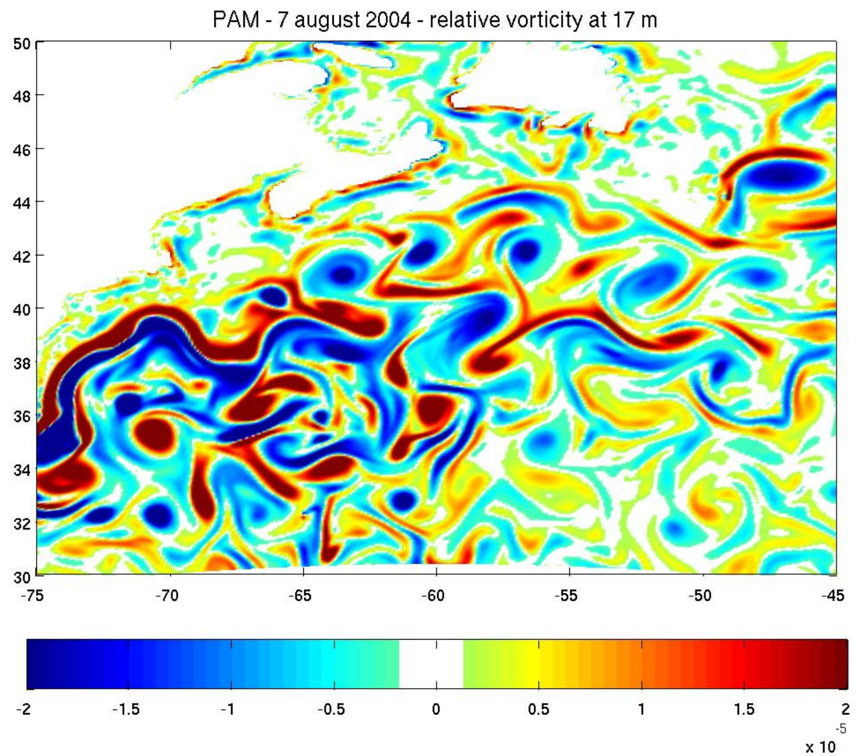
PAM - 7 august 2004 - relative vorticity at 17 m
50
48
46
44
42
40
38
36
34
32
30
-75
-70
-65
-60
-55
-50
-45
-2
-1.5
-1
-0.5
0
0.5
1
1.5
2
x 10
-5

Isopycnal mixing of tracers

Parameterizations used in models are not based on observations or theories of the mesoscale and submesoscale eddy field.

Isopycnal laplacian is probably better than horizontal biharmonic, but the coefficient should be spatially variable

What is the dependency with depth?

4 - Lateral momentum mixing

-No simple physical basis for parameterizations.

-Theory and observation for the submesoscale: ?

-Theory and observations for the effect of mesoscale eddies:

- concentration of momentum into eastwards jets
- generation of mean flow following f/h contours

Eddy effects on a zonal jet (1)

Streamfunction in the top layer, instantaneous

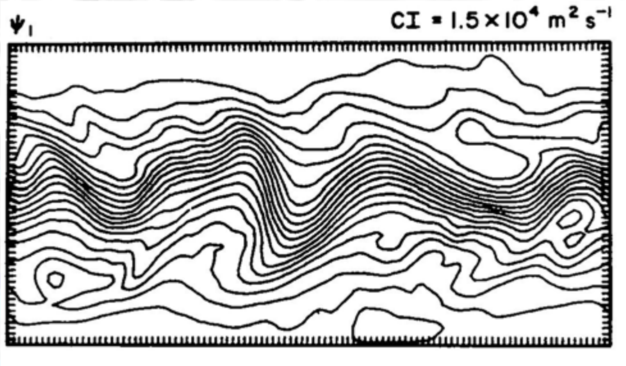

Temperature perturbation

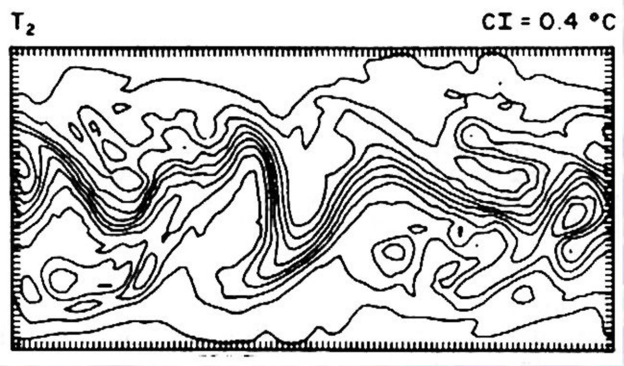

Numerical study of McWilliams and Chow (JPO, 1981)

100 points x 50 points QG model
3 layers, periodic channel
Length 2000km, width 1000km
First Rossby radius 32.4 km

Wind forcing in the top layer :

$$\tau = \sin(\pi y/L_y)$$

Eddy effects on a zonal jet (2)

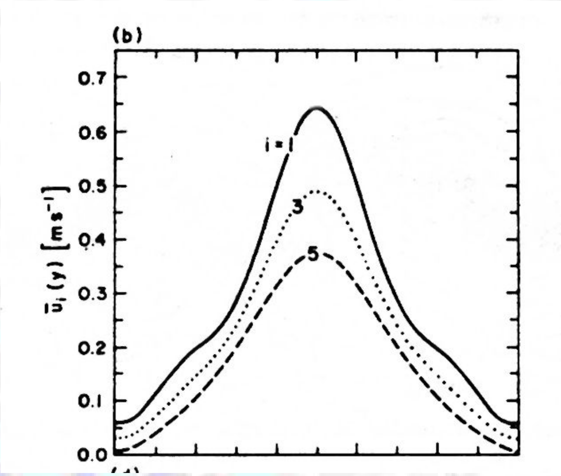

Mean zonal velocity in three layers

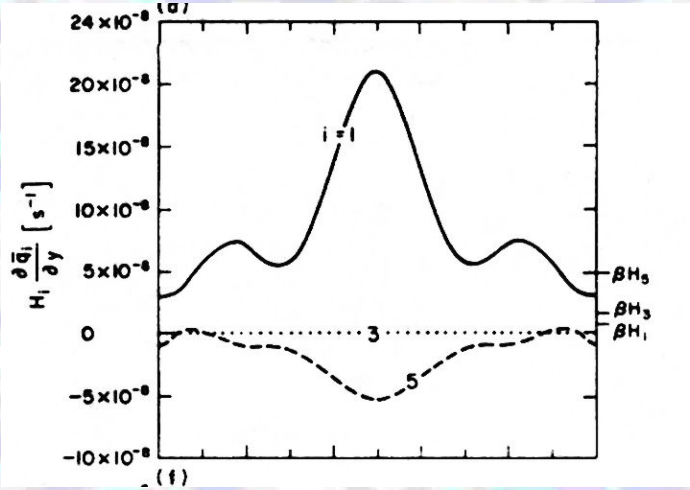

Mean potential vorticity in three layers

$Q = \nabla\psi^2 + \beta y$

$+ \partial/\partial z\ (f^2/N^2)\ \partial\psi /\partial z$

Eddy effects on a zonal jet (3)

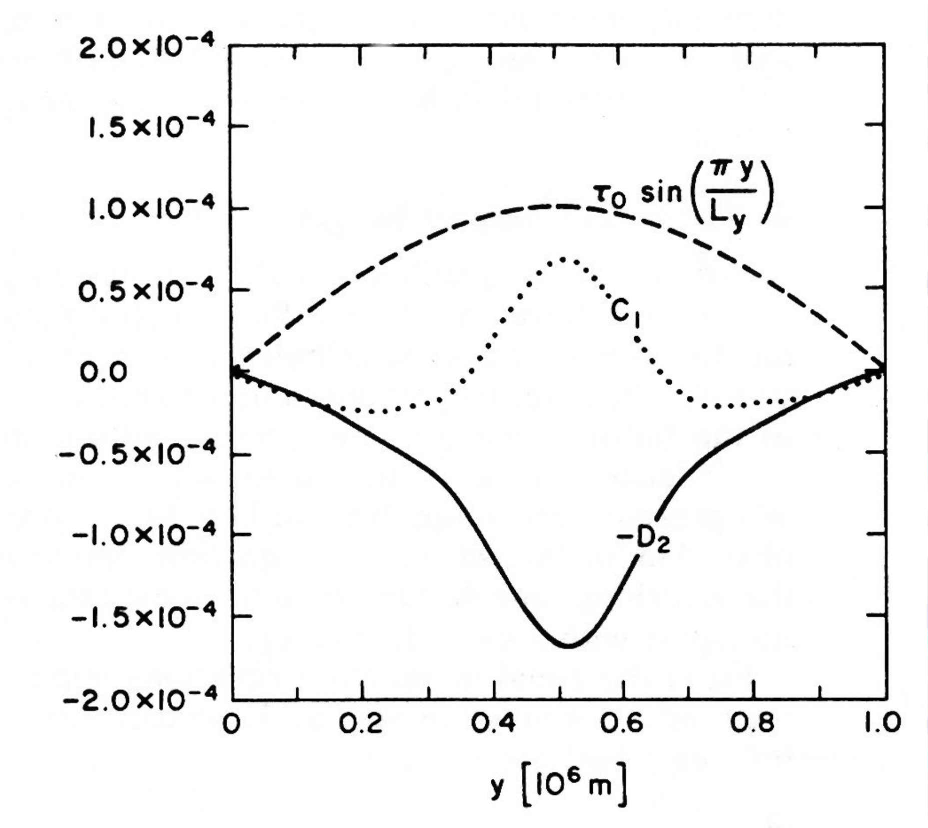

Momentum balance in layer 1

C = ∂/∂y (u'v') : Reynolds stress

Eddy effects on a zonal jet (4)

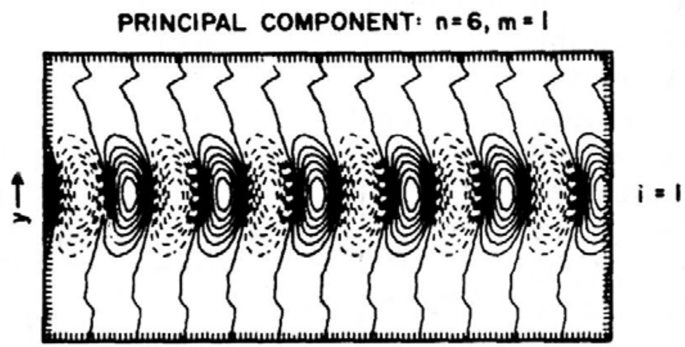

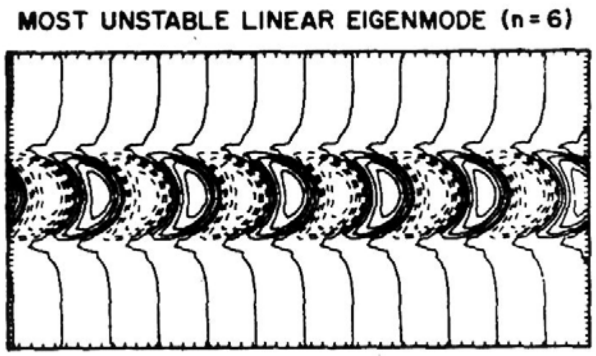

Eastward flow on a β –plane:

Concentration of momentum by eddy fluxes

Example: the atmospheric jet stream.

Eddy effects on a zonal jet (5)

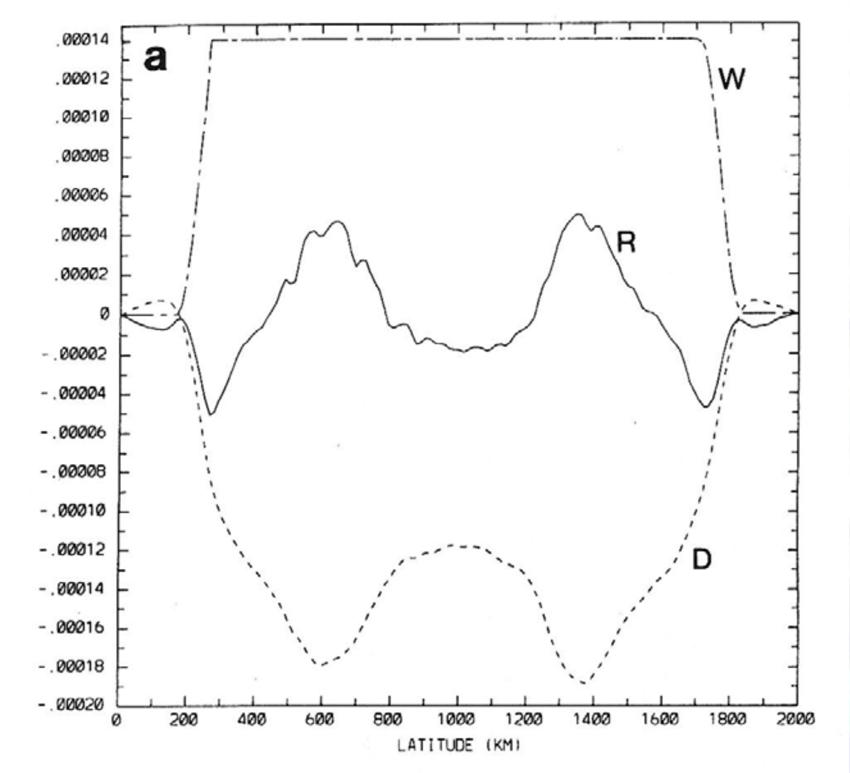

Consequense: the meridional width of the jets is set by turbulence, not by the forcing scale

Treguier and Panetta (JPO, 1994)

Wide channel + wide forcing

Two jets.

Eddy effects on a zonal jet (6)

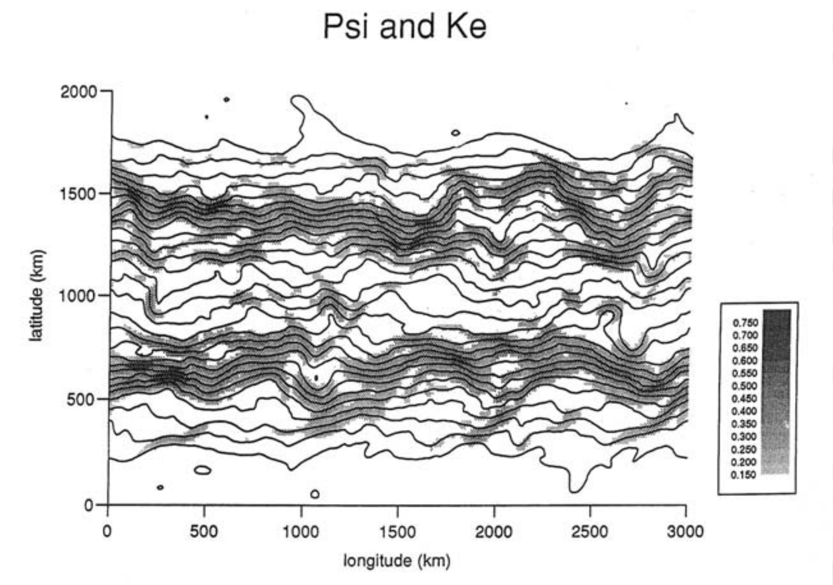

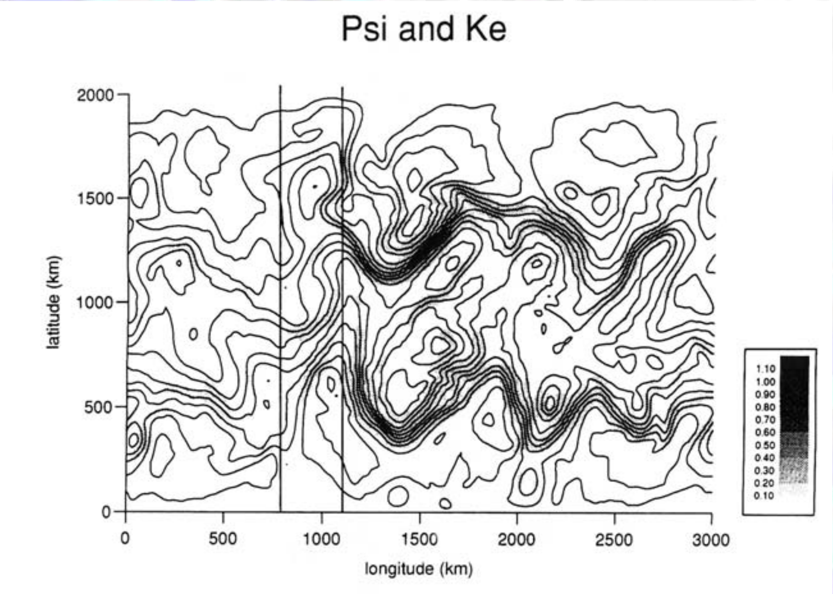

Large scale topography also has a very strong influence

Top: flat-bottom channel

Bottom: channel with a meridional gaussian ridge.

Neptune effect

In the presence of a large scale PV gradient, eddies tend to generate a flow along f/h contours (Rhines, Bretherton and Haidvogel, Holloway…)

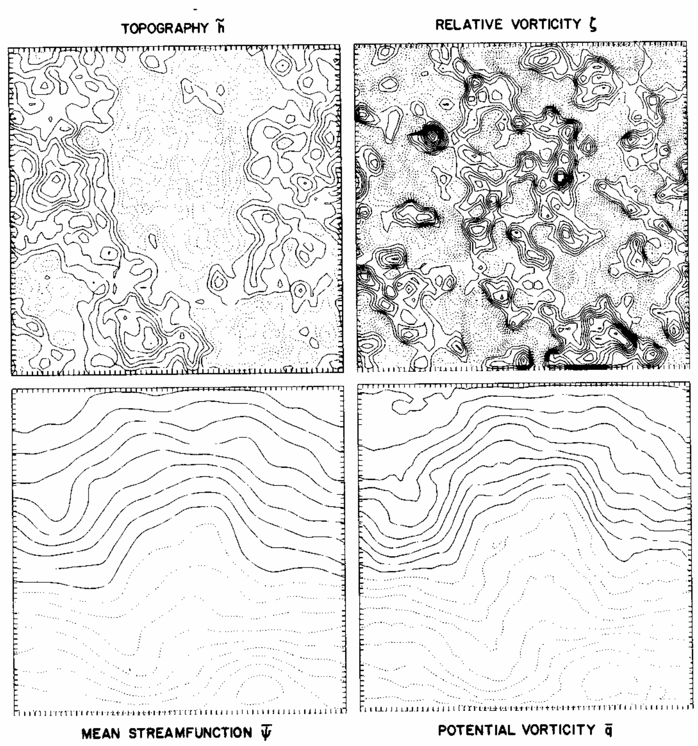

Figure 8 Time-averaged fields for experiment B3. Contour intervals are 40 m for the topography $3\times10^{-7}\,s^{-1}$ for the relative vorticity $\bar{\zeta}$, $5000\,m^2\,s^{-1}$ for the streamfunction $\bar{\psi}$, and $10^{-6}\,s^{-1}$ for the potential vorticity $\bar{q}=\bar{\zeta}+\tilde{h}$.

Generation of time-mean currents in a barotropic QG channel with stochastic uniform forcing (Treguier, 1989)

Neptune effect

The amplitude of the rectified flow depends in a non-monotonic way on the different parameters

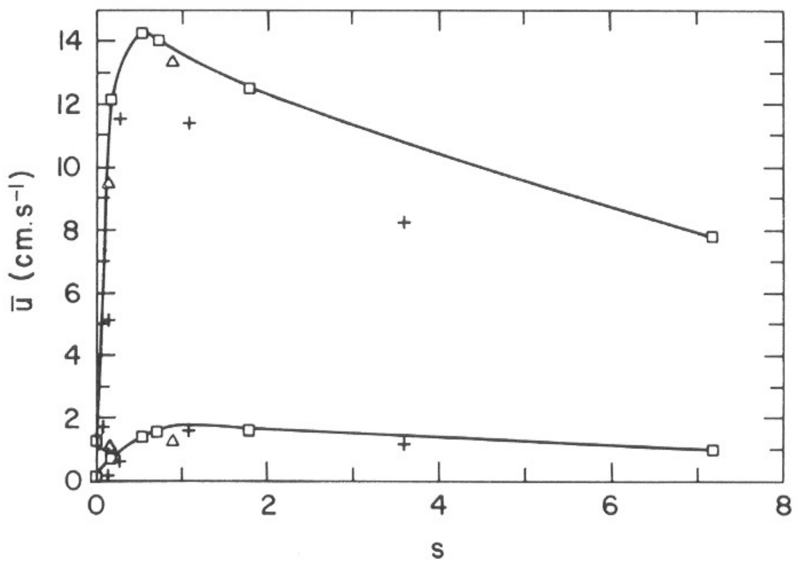

Figure 11 Steady westward flow $\bar{U}$ as a function of $S = \beta H / f_0 \alpha$. The lower curve is for experiment in Tables 4 and 5 with $\tau_0 = 2.5$ and the upper curve for $\tau_0 = 15$. The squares along the curves are for experiments in which β varies. Crosses are for experiments in which δ varies, and triangles for experiments in which the topographic spectrum varies.

The Zapiola Anticyclone in the Argentine Basin : An circulation driven by eddy-topography interactions

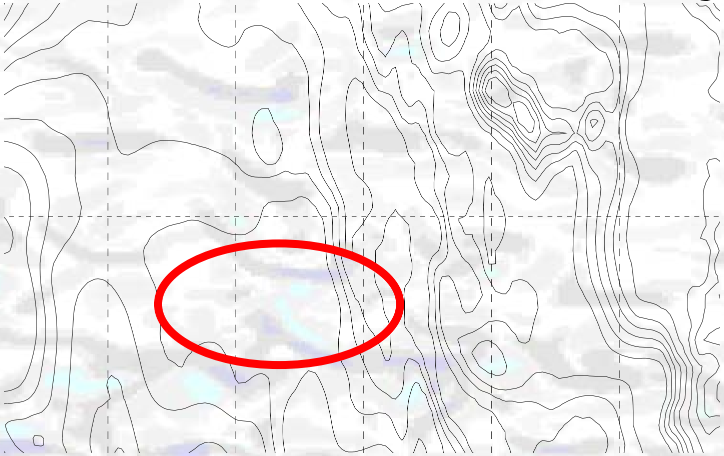

Bottom Topography

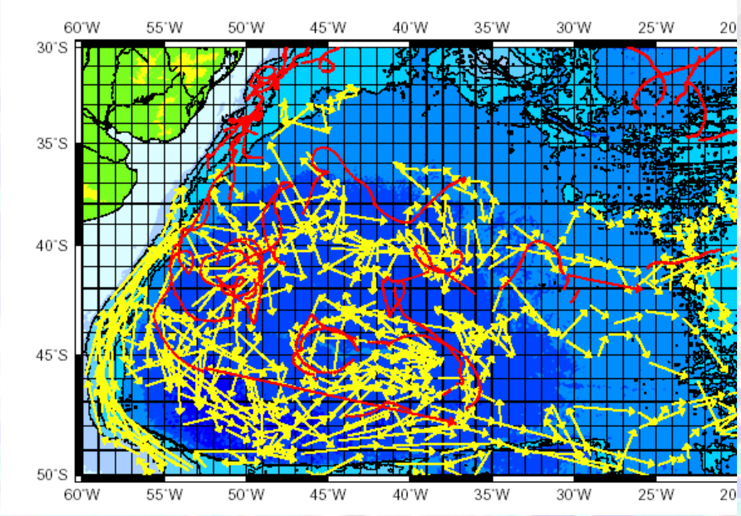

Marvor and Alace floats
(Ollitrault, Davis...)

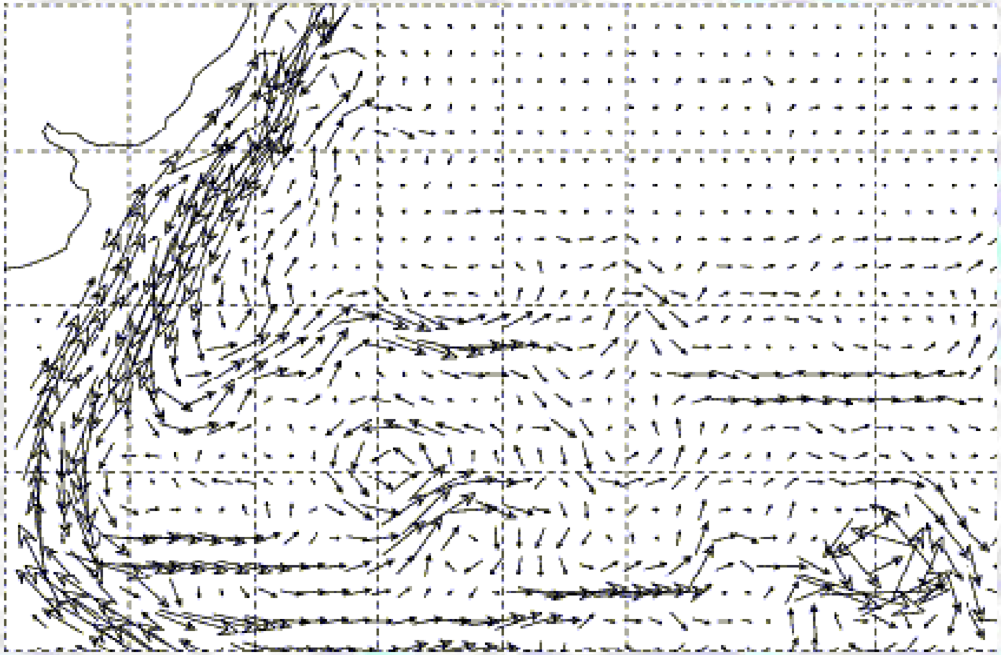

Mean circulation, 350 m
SPEM 1/3° model, σ coordinate
(de Miranda et al., 1999)

Mersea 1 lateral parameterizations

	PSY2	FOAM	MSF1	MFS2
Diffusivity	biharm	laplacian	biharm	biharm
ν_T	$3\ 10^9$	$100\ m^2s^{-1}$	$1.5\ 10^{10}$	3.10^9
orientation	hor	Iso+backg.	hor	hor
Viscosity				
$\nu_m\ (m^4s^{-1})$	$9\ 10^9$	$2.6\ 10^9$	$5.\ 10^9$	5.10^9
$\nu_m\ (m^2s^{-1})$		30		

Lateral momentum mixing

Parameterizations actually used:

- laplacian
- biharmonic
- smagorinsky
- dependence of the coefficient on the grid scale
- Anisotropic viscosity

Anisotropic viscosity

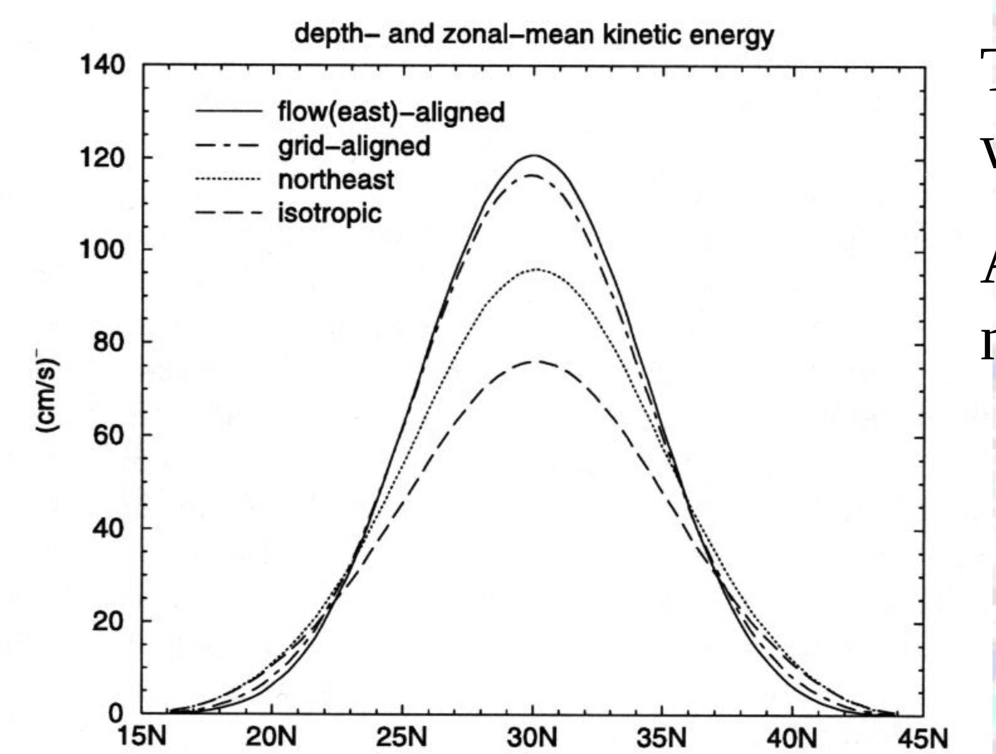

Smith and Mc Williams, 2003

Test in a zonal channel flow, wind driven.

Anisotropic viscosity allows a narrower and stronger jet.

Anisotropic viscosity

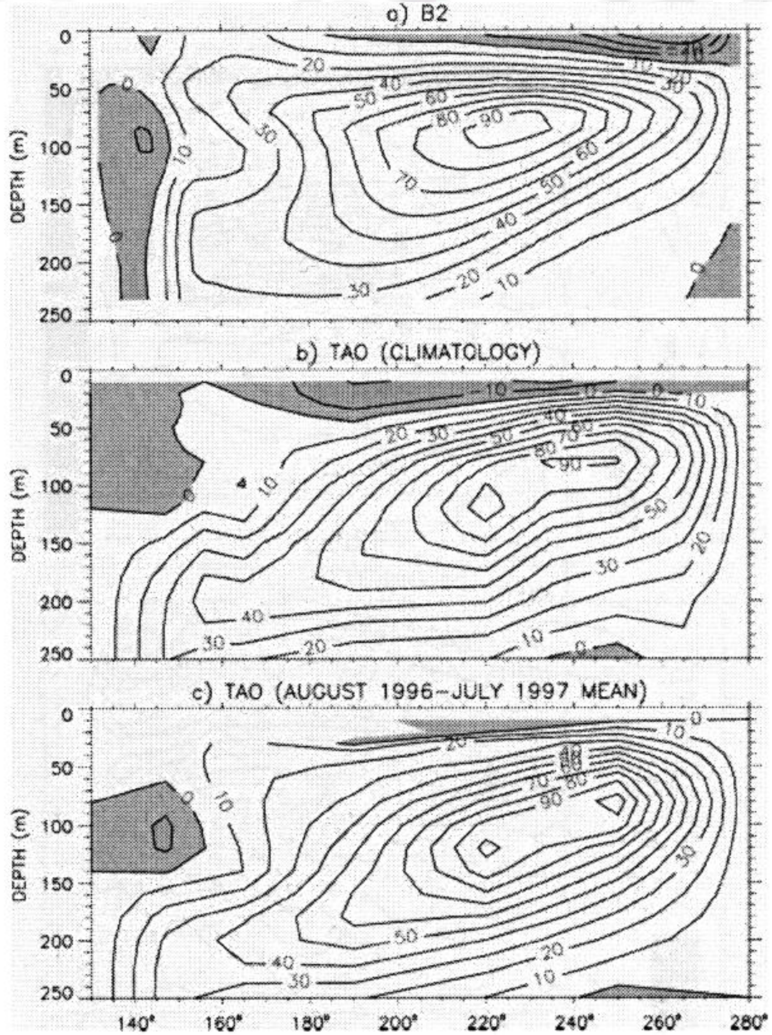

FIG. 2. Zonal sections across the Pacific of zonal velocity at the equator: (a) annual average of case B2, (b) TAO current meter cli-

Large et al, 2001

Test of a zonal/meridional anisotropic viscosity in a coarse resolution model (2°).

Improvement of the Equatorial undercurrent.

Some numerical noise remains.

Lateral viscosity: conclusions

We need theories;

Cascade of enstrophy to small scale and energy to large scales: need a source of energy at large scales? (anticipated vorticity method).

5 - Advective effect of mesoscale eddies

Effect pointed out by Gent and Mc Williams (1990, 1995)

Mesoscale eddies have an effect on the density field!

Example in the case of restratification after convection

(Chanut, 2003)

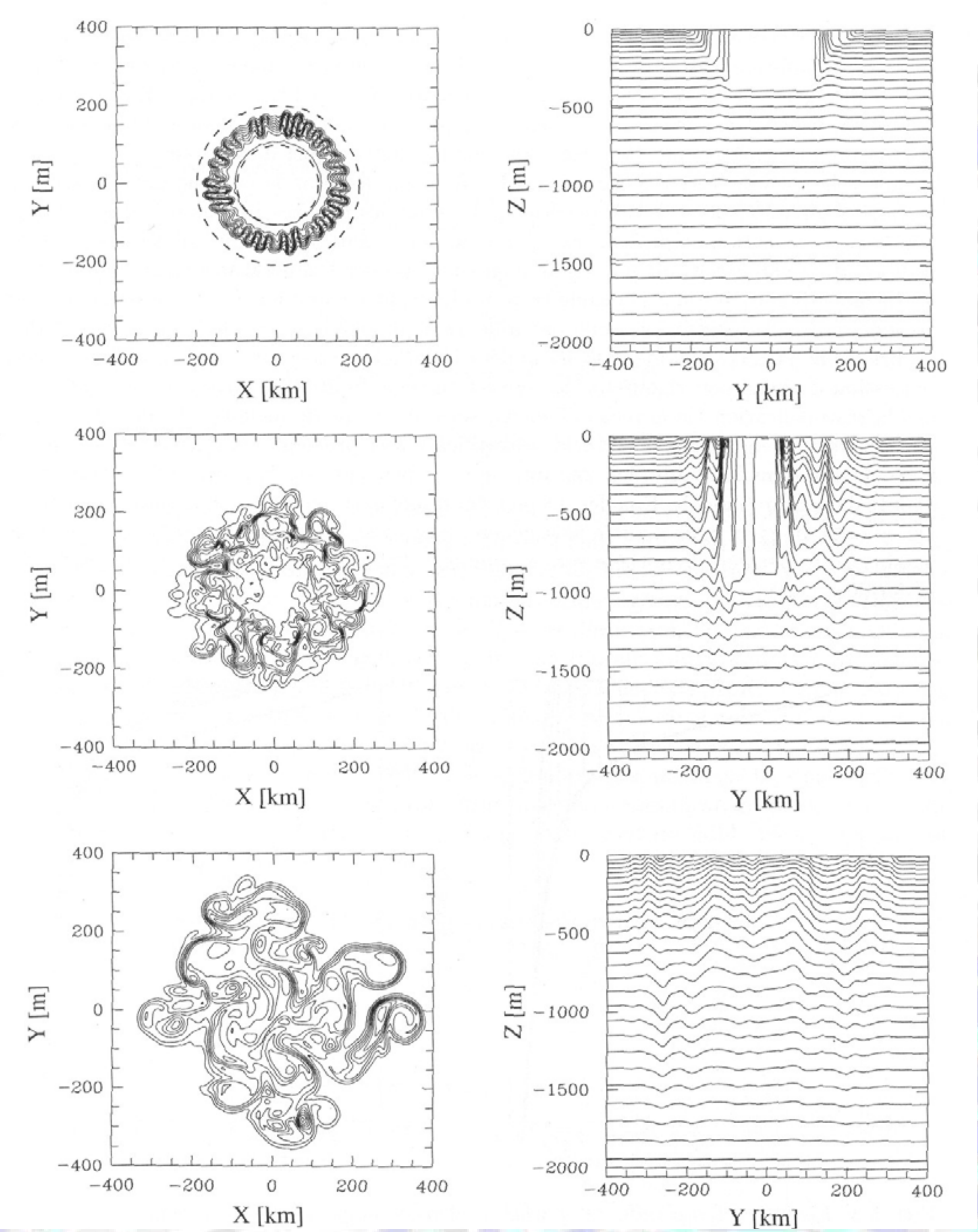

Eddy-driven restratification (1)

The convective chimney is baroclinically unstable: eddies develop and drive restratification

(Chanut, 2003)

Eddy-driven restratification (2)

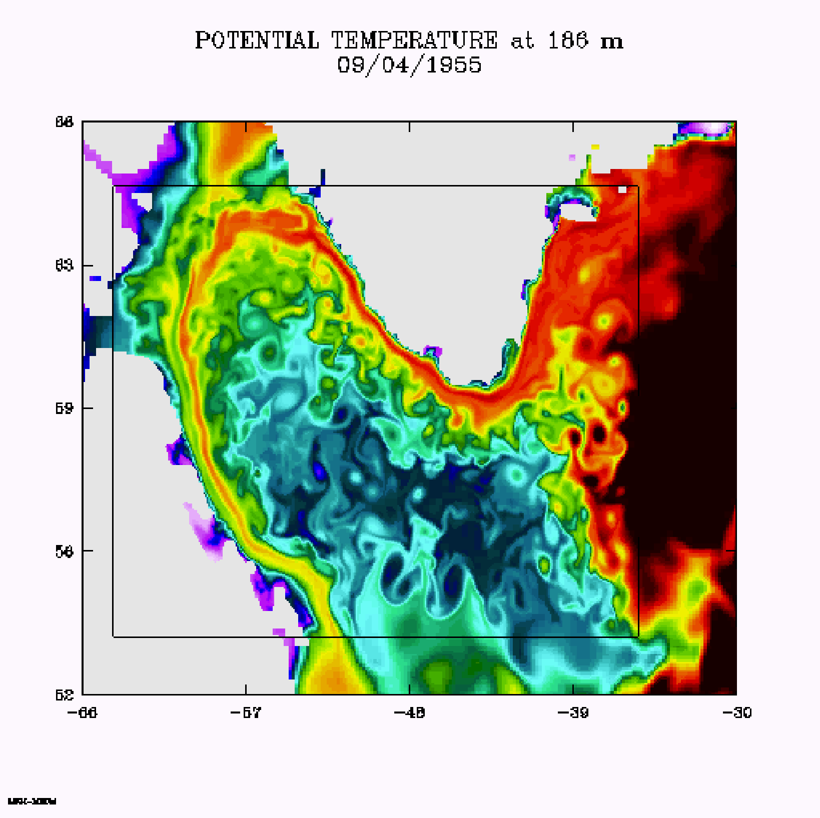

Application to the Labrador Sea using the AGRIF grid refinement (Chanut and Barnier)

Eddy-driven restratification (3)

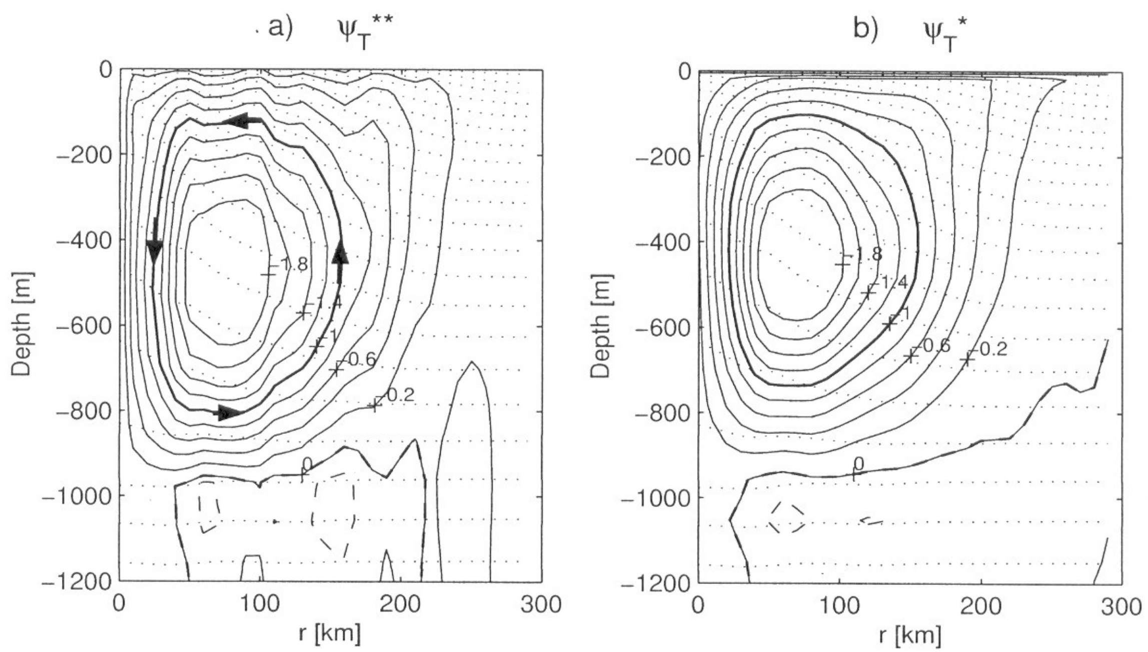

FIG. 6.8: *Fonctions de courant associées aux vitesses de transport [$m^2.s^{-1}$] à t=246 jours (CI = 0.2 $m^2.s^{-1}$). a) En moyennant en coordonnées isopycnales :* $\psi_T^{**} = \int(\overline{u_r}^{\rho} + u_r^{**})d\rho$. *b) En moyennant en coordonnées z :* $\psi_T^{*} = \int(\overline{u_r} + u_r^{*})dz$. *Les isocontours de densité sont en pointillés et les flèches symbolisent le sens de la circulation.*

The effect of eddies can be viewed as an advective circulation

Local flux-gradient relationship: 1D

Fickian diffusion:

$$(w'T')_R = -\kappa \; \partial T_R / \partial z$$

Flux-gradient relationship in 2D

Case of a local flux-gradient relationship in 2D:

One may assume the mixing tensor to be diagonal, but mixing along the two directions may not be the same:

$$[\, v'T',\ w'T' \,] = K \ \nabla T$$

$$K = \begin{vmatrix} K_y & 0 \\ 0 & K_z \end{vmatrix}$$

$K_y \gg K_z$

More general mixing tensor in 2D

LOCAL flux-gradient relationship

$$F = \overline{u'q'} = -\mathbf{K}\nabla\overline{q}.$$

mixing tensor in two dimensions:

$$\mathbf{K} = \begin{bmatrix} K_{yy} & K_{yz} \\ K_{zy} & K_{zz} \end{bmatrix}.$$

Dynamic eddy effect:
ANTISYMMETRIC component of tensor

$$\mathbf{L} = \begin{bmatrix} 0 & \gamma \\ -\gamma & 0 \end{bmatrix}.$$

Eddy induced velocities

Turbulent flux due to antisymmetric tensor:

$$\overline{v'q'} = -\gamma\frac{\partial q}{\partial z}$$
$$\overline{w'q'} = \gamma\frac{\partial q}{\partial y}$$

The flux divergence:

$$\nabla F = -\frac{\nabla\gamma}{\partial y}\frac{\nabla q}{\partial z} + \frac{\nabla\gamma}{\partial z}\frac{\nabla q}{\partial y}.$$

is advection by the eddy-induced velocity:

$$v^* = \partial\gamma/\partial z,$$
$$w^* = -\partial\gamma/\partial y.$$

Parameterization of eddy-induced velocities

Gent and McWilliams parameterization: advection velocity as a function of mean density $\overline{\rho}$.

$$u^* = -\frac{\partial}{\partial z}\left(\kappa\frac{\partial\overline{\rho}/\partial x}{\partial\overline{\rho}/\partial z}\right);$$

$$v^* = -\frac{\partial}{\partial z}\left(\kappa\frac{\partial\overline{\rho}/\partial y}{\partial\overline{\rho}/\partial z}\right);$$

$$w^* = \frac{\partial}{\partial y}\left(\kappa\frac{\partial\overline{\rho}/\partial y}{\partial\overline{\rho}/\partial z}\right) + \frac{\partial}{\partial z}\left(\kappa\frac{\partial\overline{\rho}/\partial x}{\partial\overline{\rho}/\partial z}\right) \quad (1)$$

Eddy-driven restratification (4)

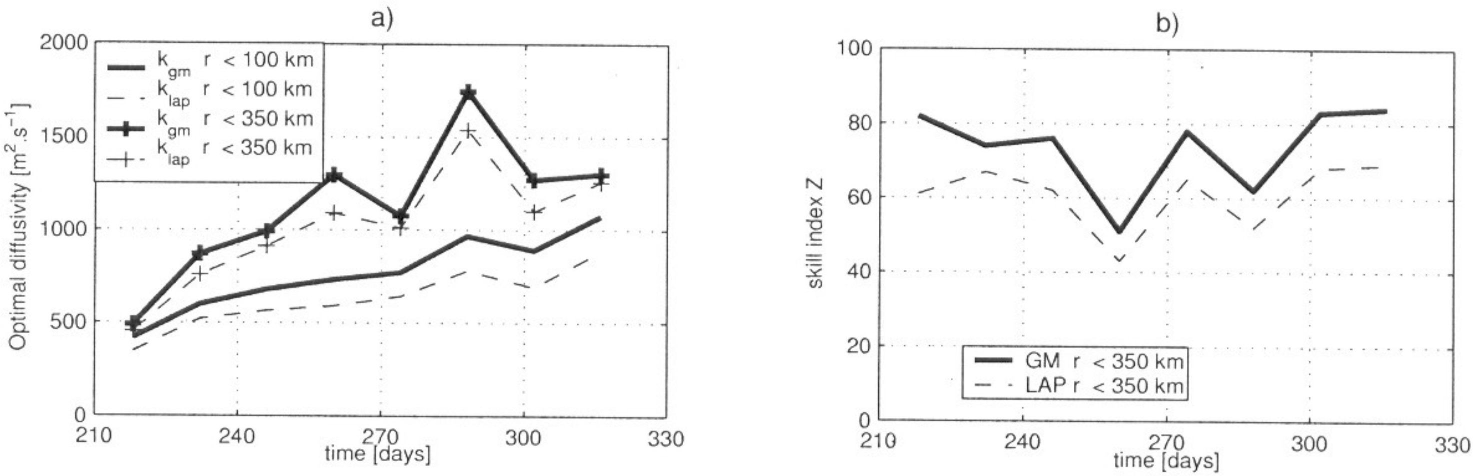

FIG. 6.11: *a) Coefficients optimums pour GM (trait plein) et le Laplacien (pointillés) en fonction du temps et suivant la zone d'estimation : $r < 350$ km et $r < 100$ km (croix). b) Indice de performance Z pour chacune des paramétrisations et pour $r < 350$ km.*

The mixing coefficients needed for GM or horizontal diffusion are large in teh case of convective chimneys: order 1000 $m^2 s^{-1}$.

5 - Advective effect of mesoscale eddies

Effect pointed out by Gent and Mc Williams (1990, 1995)

Advective flux or skew flux (Griffies 2004)

Does a GM parameterization improve an ocean model?

Does a variable eddy coefficient help?

Do we need a GM parameterization in eddy permitting models?

Challenge: eddies and the surface layer!

Eddy-induced velocities in a zonal channel

Treguier, 1999

Large values of eddy-induced velocity

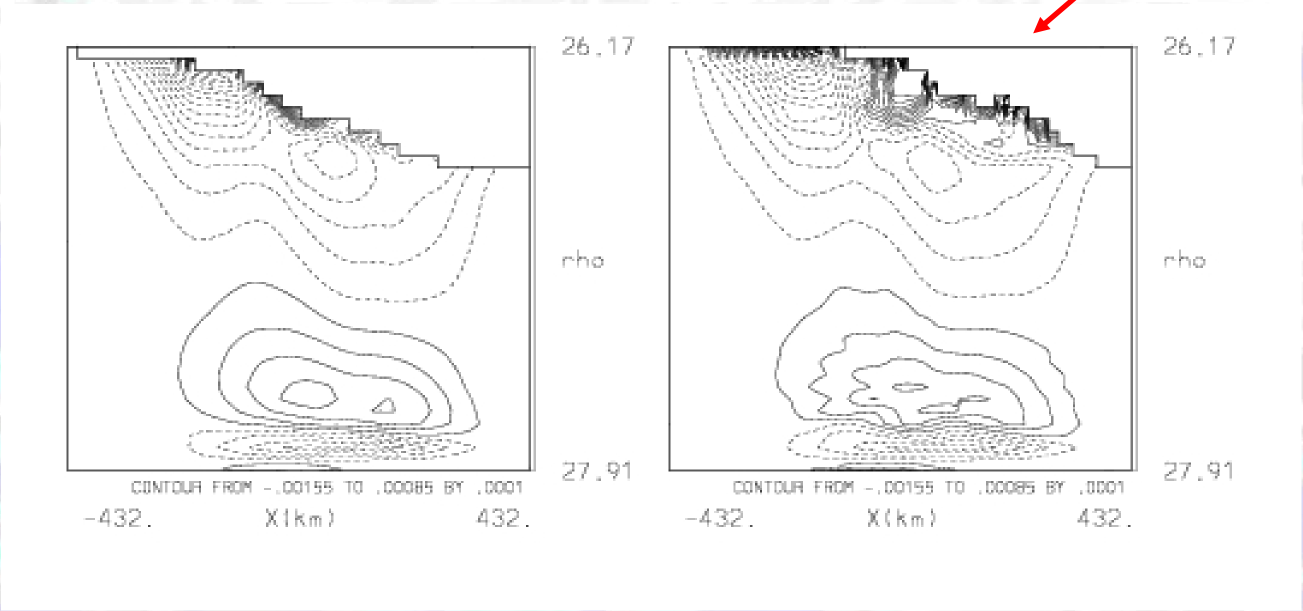

V* (QG) as a function of y and ρ

The density domain corresponds to the time-averaged ρ.

V* (isopycnic) as a function of y and ρ

The density domain corresponds to all possible values of ρ.

Conclusions: parameterizations

•Ideal case: physics, observations/lab experiments, validation against a complete model

•Improvements at the boundaries: surface and bottom

•Parameterizations of mesoscale eddies: hopeless? (non local transport)

- coarse resolution climate models give useful information even without a good representation of eddies

- Forecast models need to resolve the eddies and better submesoscale parameterizations